Frequency Conversion

- Frequency conversion-Hamiltonian [1]

$$\hat{\mathcal{H}} = \mathrm{i}\hbar\kappa A_p\, \hat{a}_{\mathrm{in}}\hat{a}^{\dagger}_{\mathrm{out}} + \mathrm{h.c.}$$

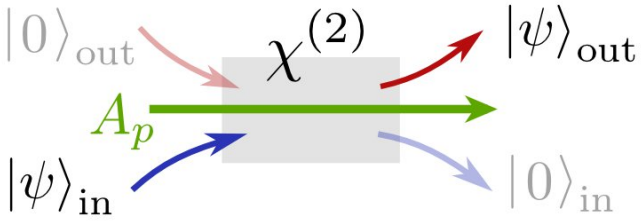

- strong pump field A_p treated classically

$$\begin{aligned}\hat{a}_{\mathrm{in}}(t) &= \hat{a}_{\mathrm{in}}(0)\cos(\kappa A_p t) - \hat{a}_{\mathrm{out}}(0)\sin(\kappa A_p t)\\ \hat{a}_{\mathrm{out}}(t) &= \hat{a}_{\mathrm{out}}(0)\cos(\kappa A_p t) + \hat{a}_{\mathrm{in}}(0)\sin(\kappa A_p t)\end{aligned}$$

- complete conversion for

$$\kappa A_p t = \frac{\pi}{2}$$

- κ depends on effective nonlinearity d_{eff}, geometry and mode overlap

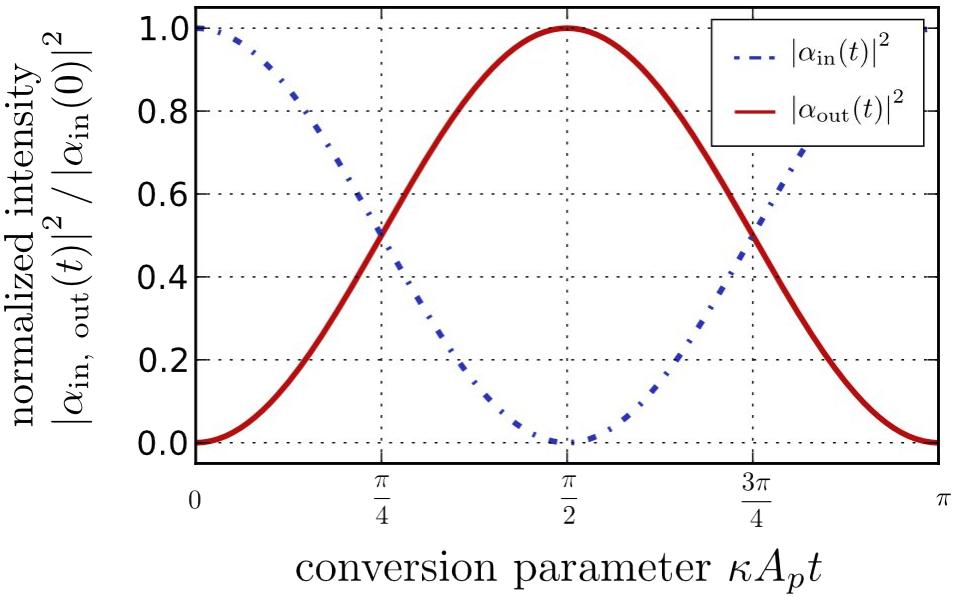

[1] P. Kumar, Optics Letters 15, 1476 (1990)

Quantum pulse gate

Dispersion-engineered frequency up-conversion

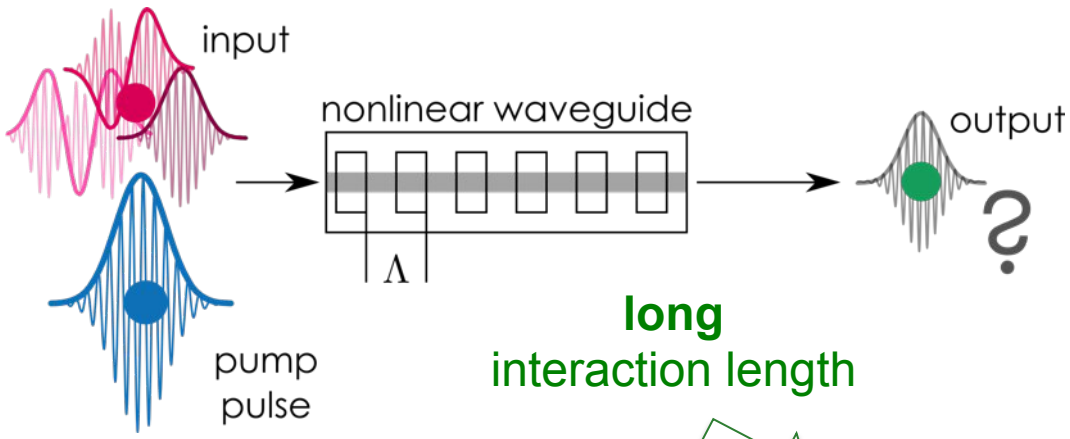

long
interaction length

Energy conservation

$$\omega_{\mathrm{p}} + \omega_{\mathrm{in}} = \omega_{\mathrm{out}}$$

Phasematching

$$\beta_{\mathrm{p}} + \beta_{\mathrm{in}} + \frac{2\pi}{\Lambda} = \beta_{\mathrm{out}}$$

$$\beta'_{\mathrm{p}} = \beta'_{\mathrm{in}}$$

group-velocity matching

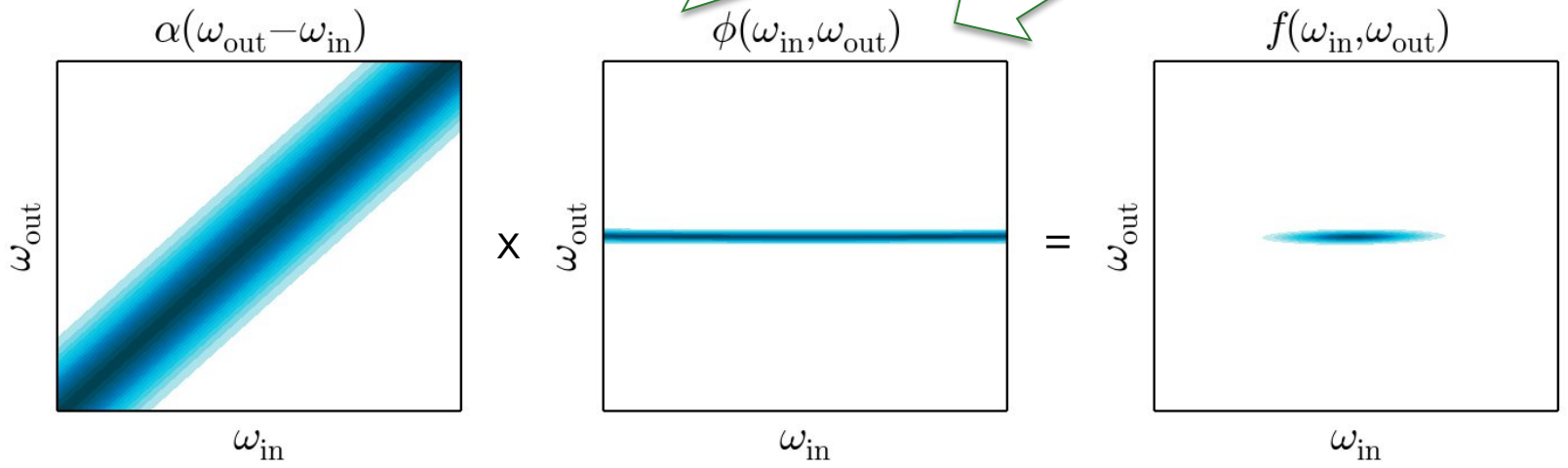

Eckstein, et al., Opt. Exp. 19, 13370 (2011)
Brecht, et al., New J. Phys. 13, 065029 (2011)

Process engineering – Pump pulse

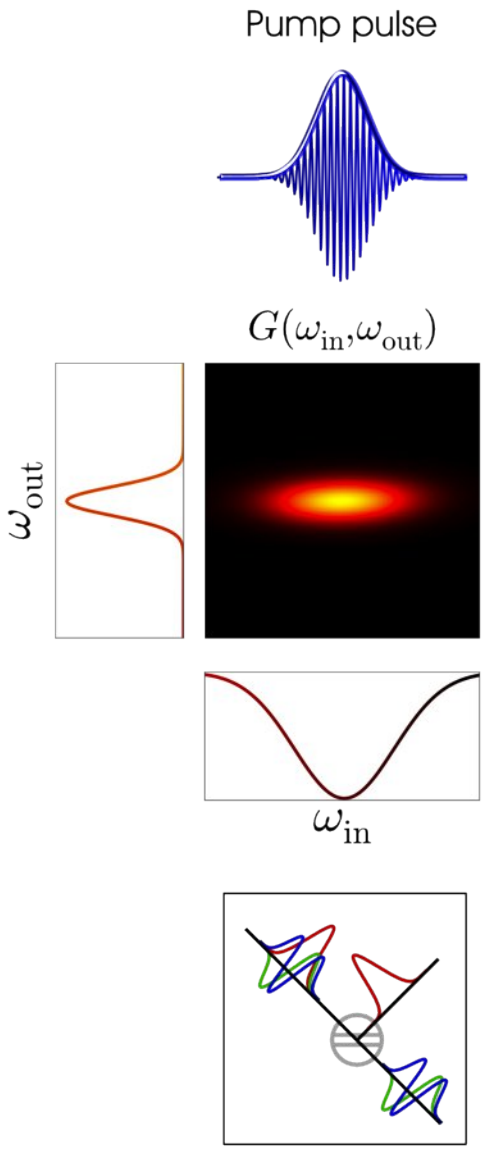

Process engineering – Pump pulse

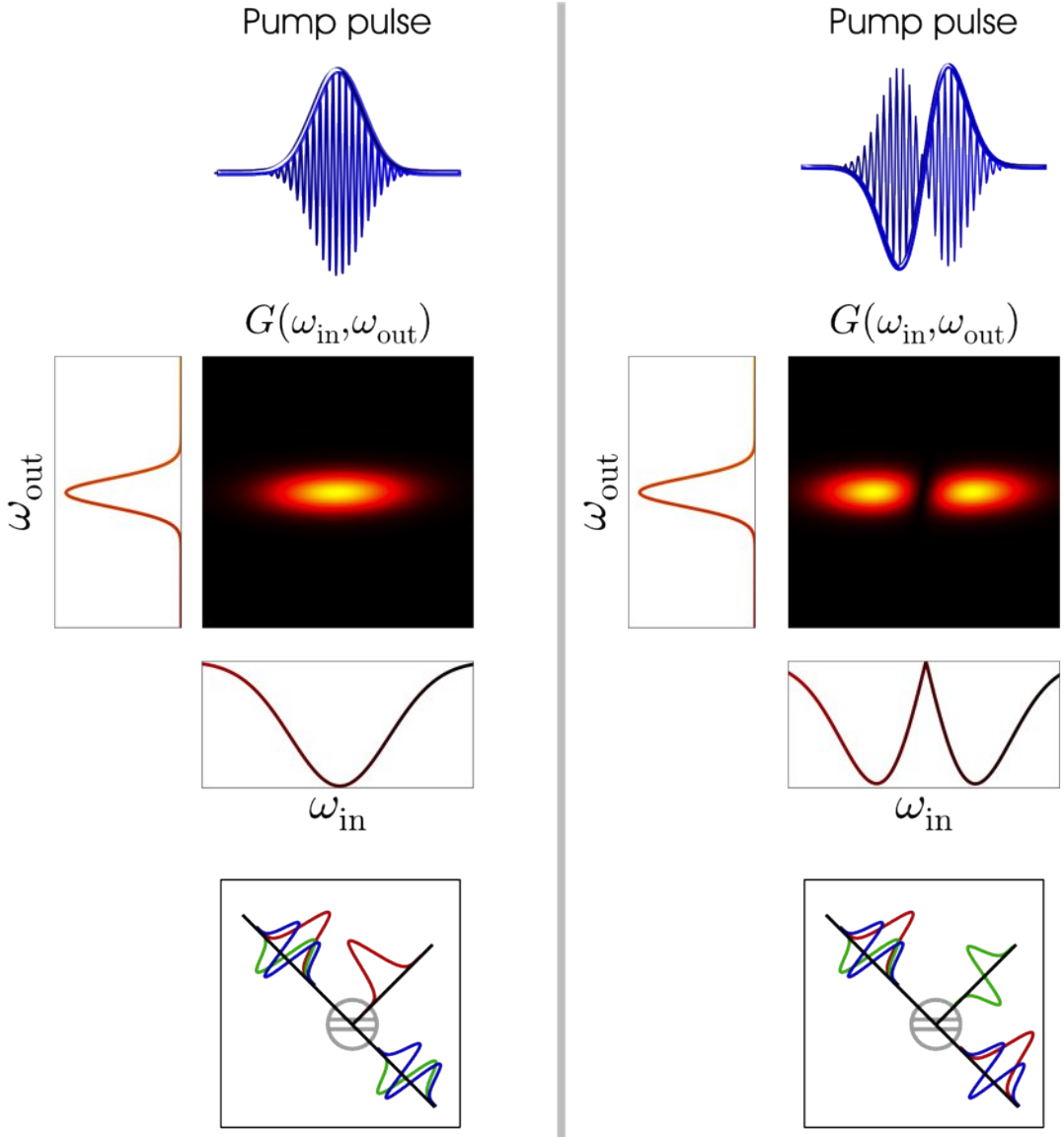

Process engineering – Pump pulse

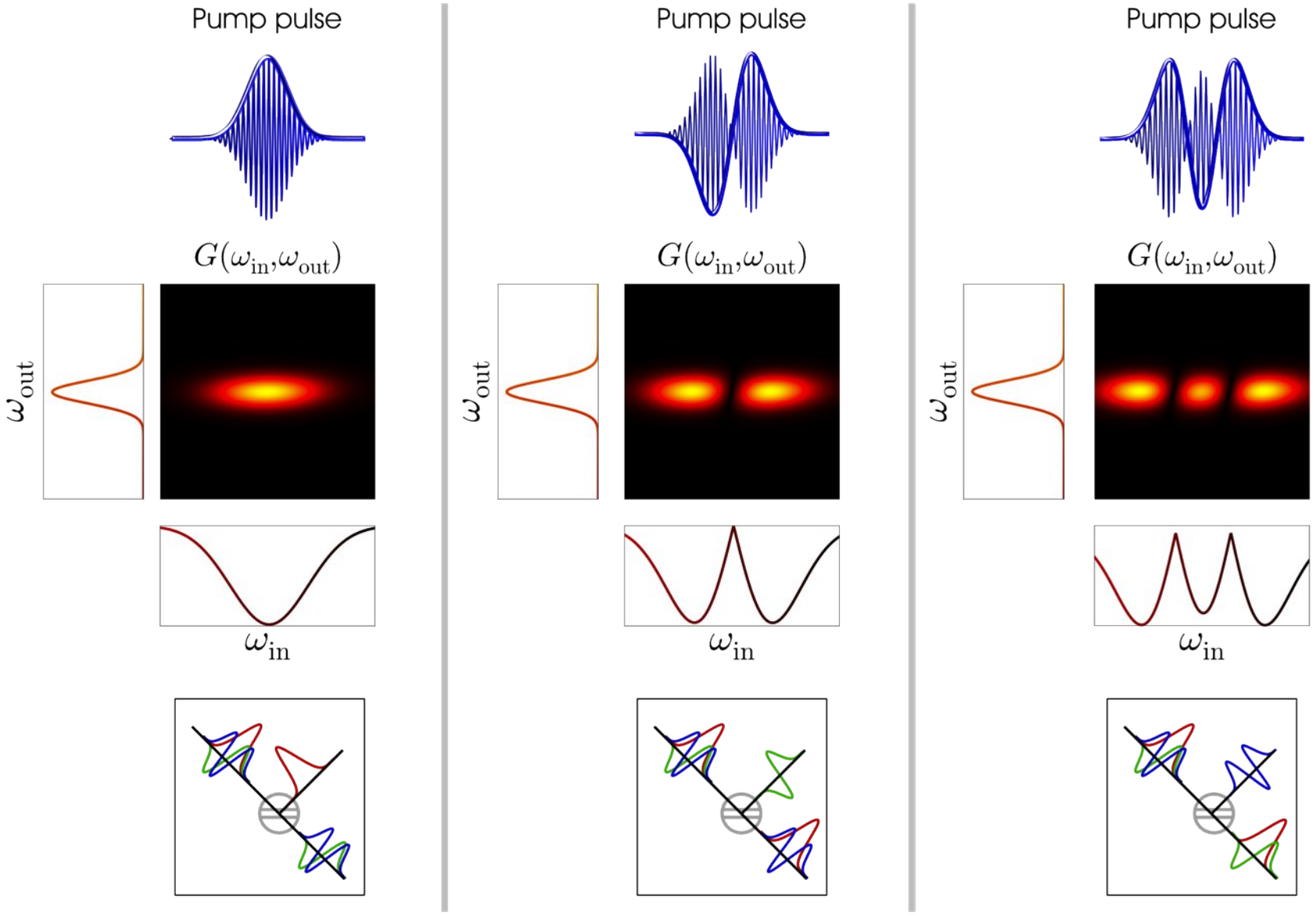

Quantum pulse gate

Dispersion engineered frequency conversion

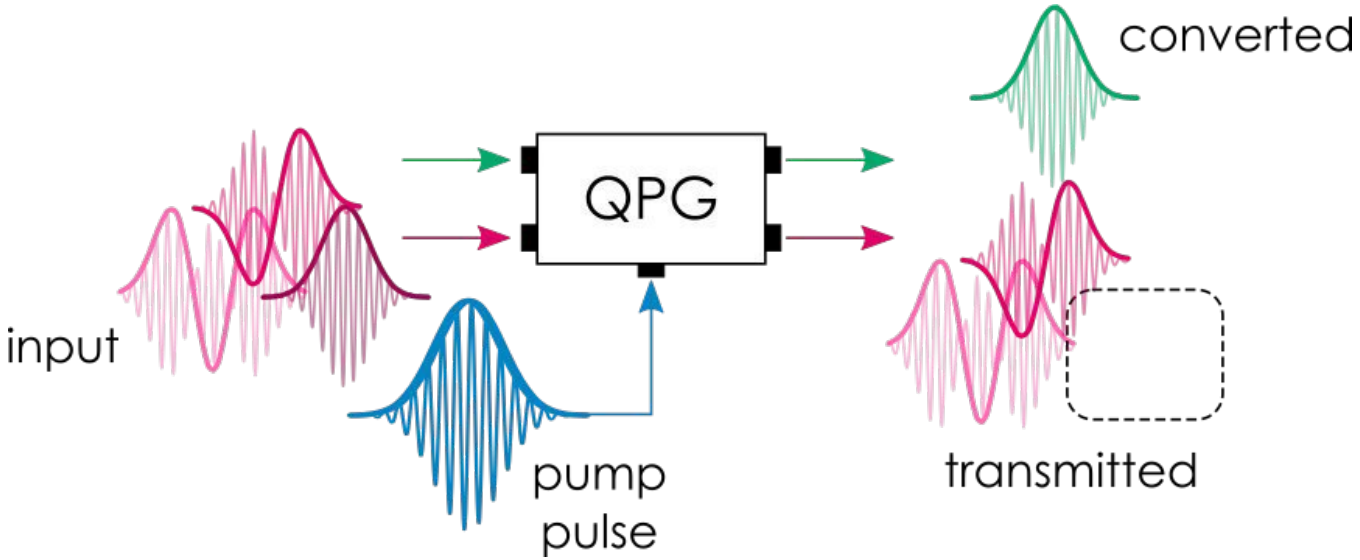

Bogoliubov transformation: beam splitter

$$\hat{A}^{(k)}_{\text{red}} \rightarrow \cos(\theta)\hat{A}^{(k)}_{\text{red}} + \sin(\theta)\hat{A}_{\text{green}}$$

$$\hat{A}_{\text{green}} \rightarrow \cos(\theta)\hat{A}_{\text{green}} - \sin(\theta)\hat{A}^{(k)}_{\text{red}}$$

efficiency adjusted with pump power

Quantum pulse gate

Dispersion engineered frequency conversion

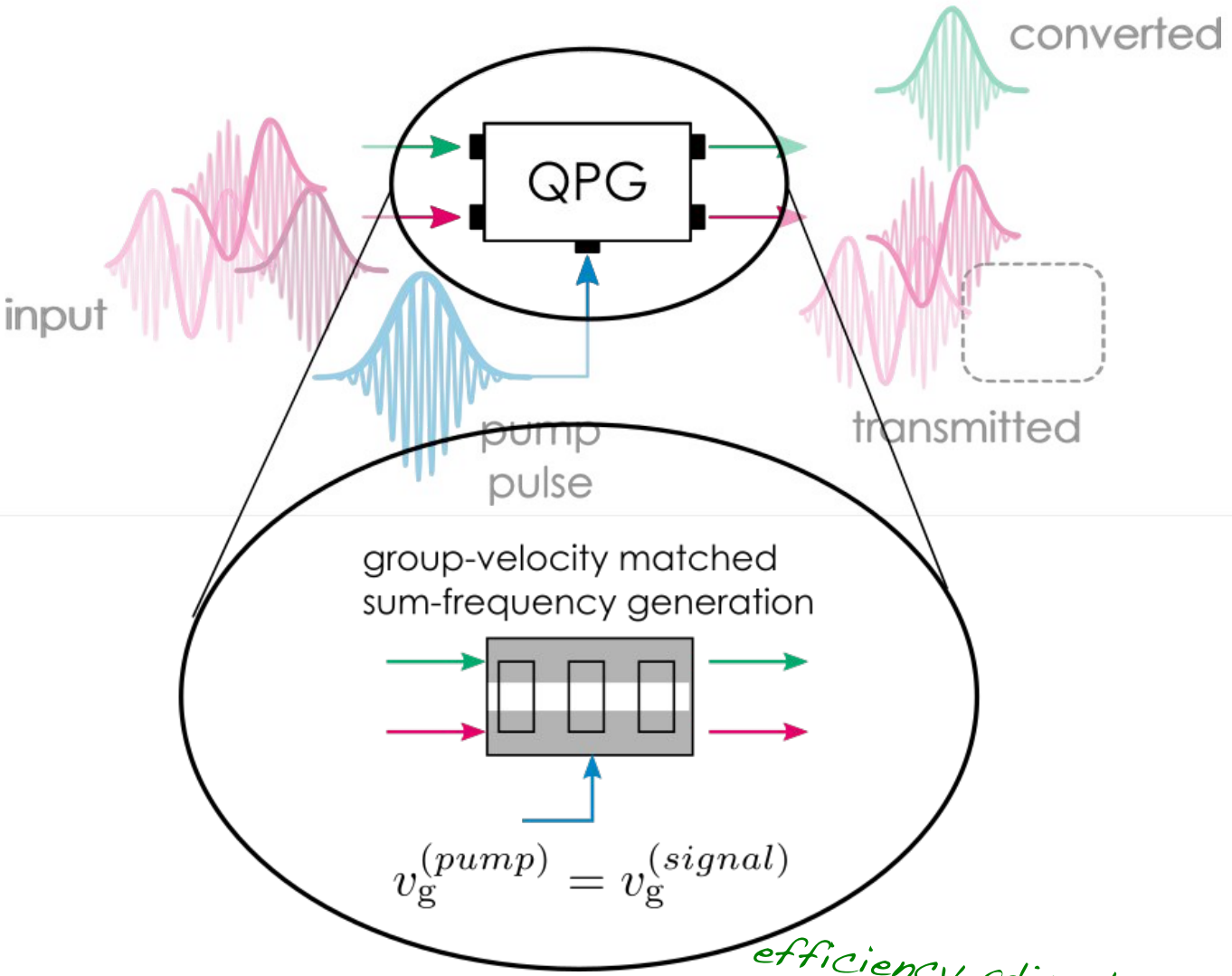

efficiency adjusted with pump power

Quantum pulse gate

Dispersion engineered frequency conversion

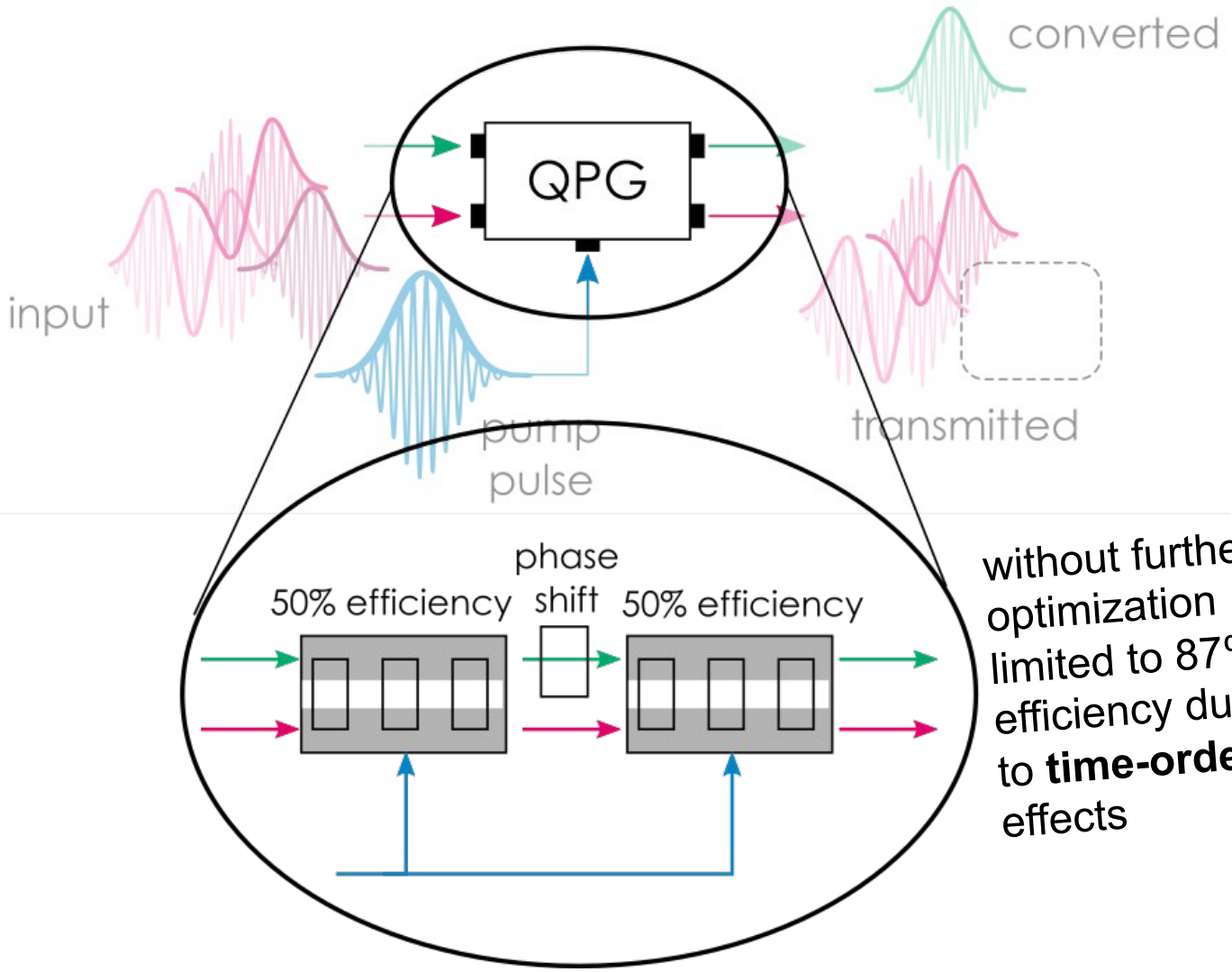

without further optimization limited to 87% efficiency due to **time-ordering** effects

Reddy, et al., Opt. Lett. 39, 2924 (2014)
Reddy, et al., Optica 5, 423-428 (2018)

PPLN waveguide

In-house manufactured periodically poled LN waveguide:

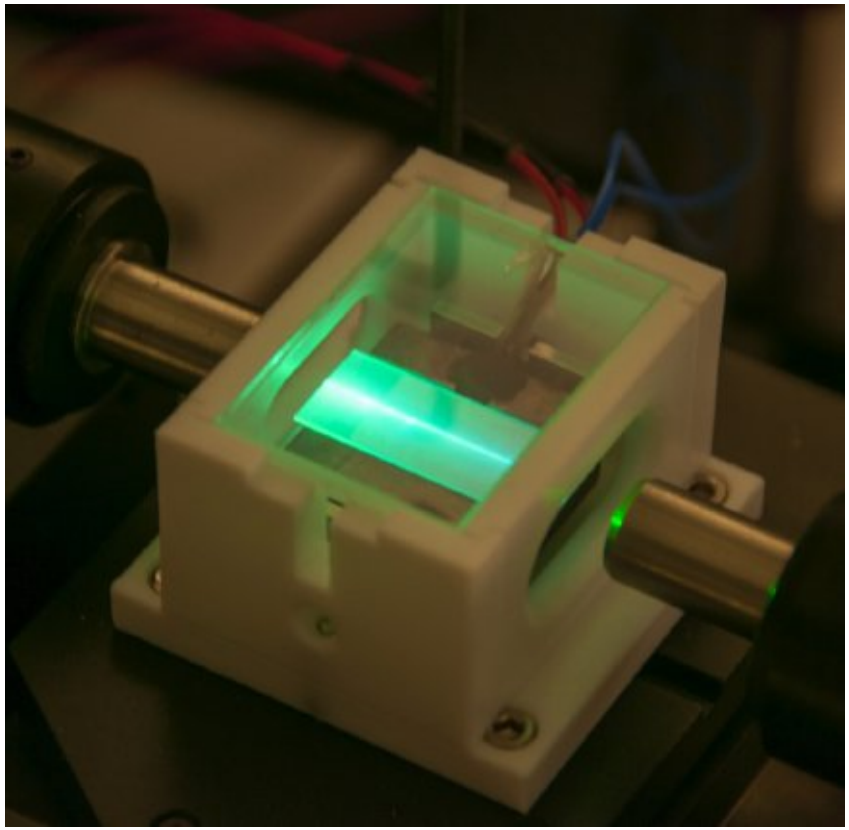

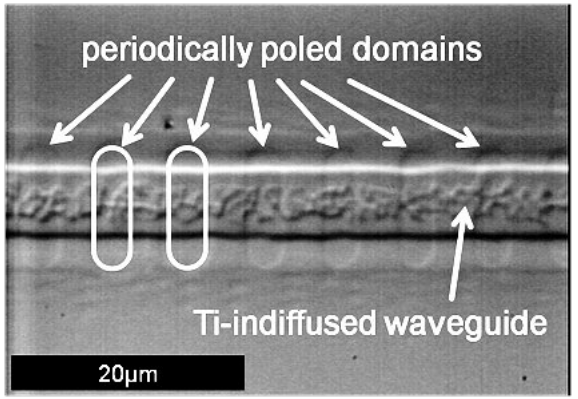

- Crystal length: 15…40 mm
- SFG: 1536nm / 874nm to 557nm
- Poling period **4.4 µm**
- Temperature stabalized at 190°C
- Bandwidth compression

Group velocity matching

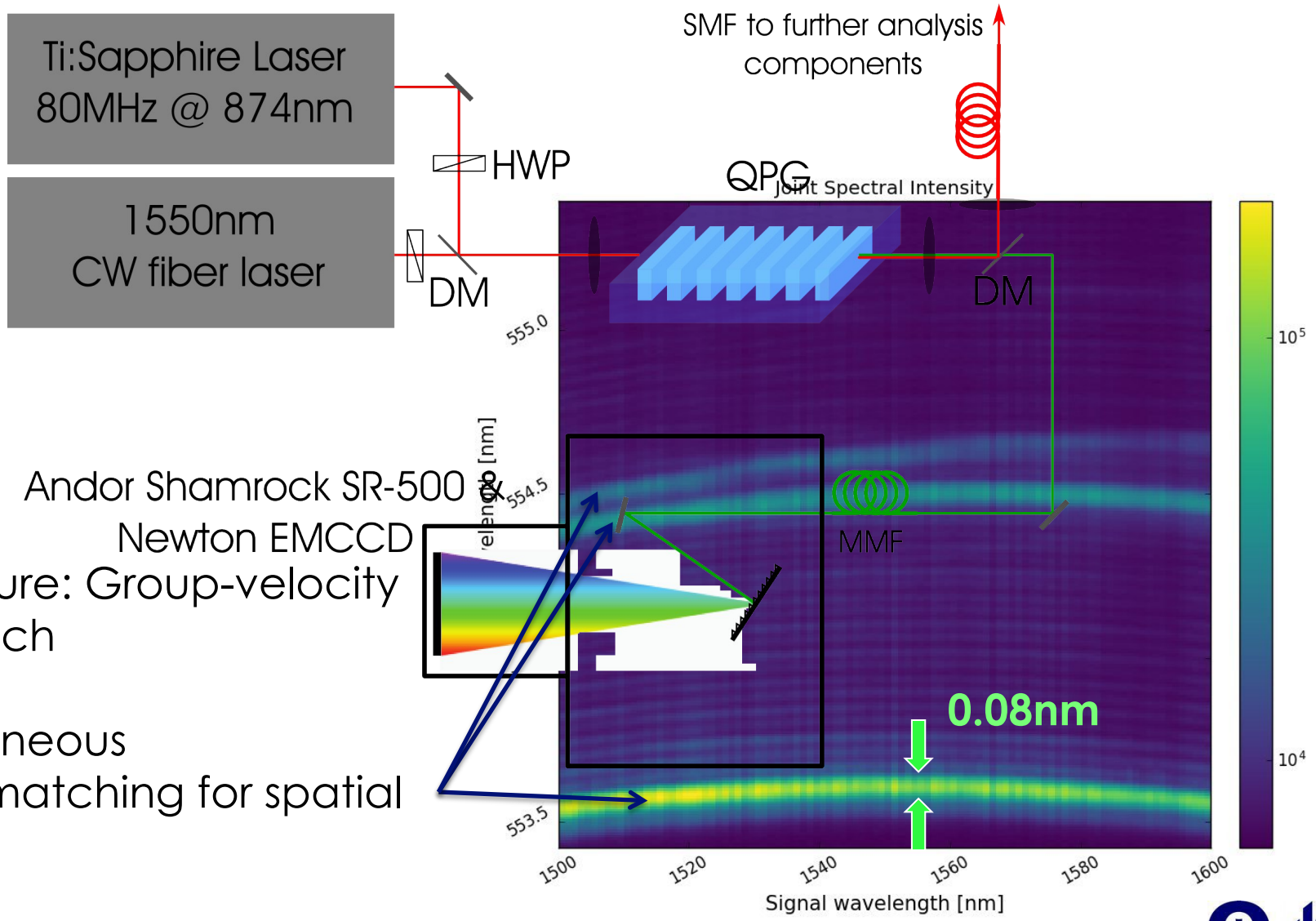

Curvature: Group-velocity mismatch

Simultaneous phasematching for spatial modes

Spectrum before vs. after conversion

Spectrum of converted photons measured on single photon sensitive spectrometer

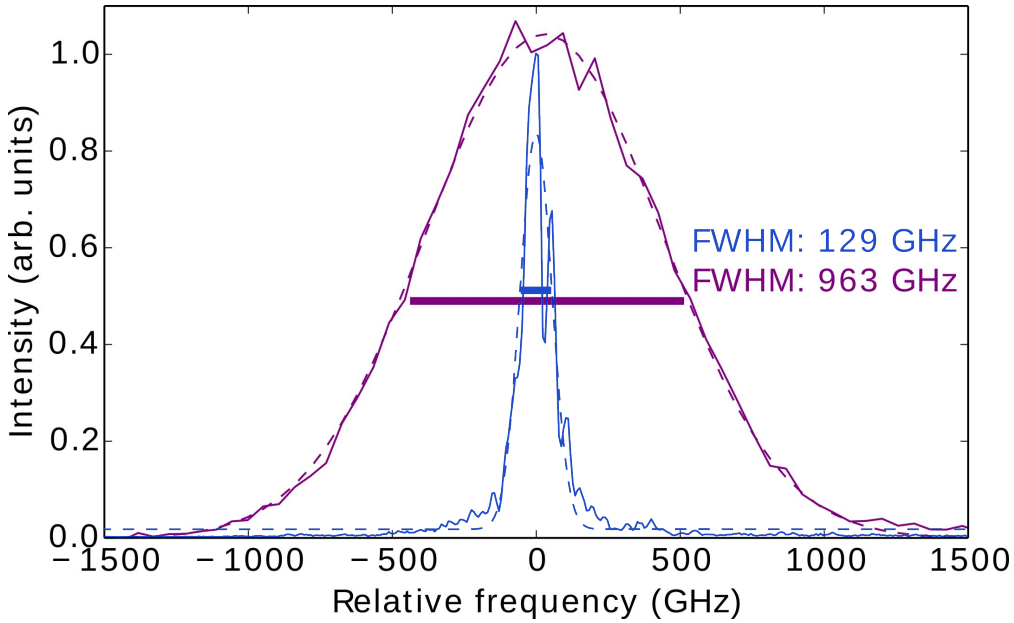

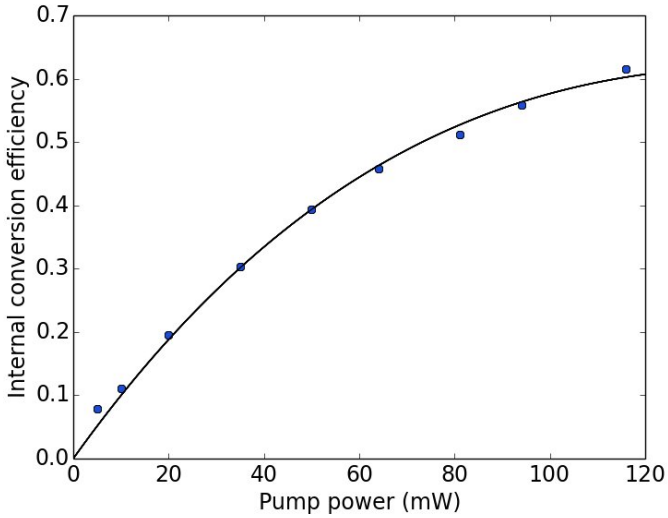

Internal conversion efficiency: 75%
External conversion efficiency: 17%

Spectrum is changed, but no implication on quantumness / efficiency

Ideal spectral filter: efficiency 13,4 %

Allgaier, et al., Nat. Com. 8, 14288 (2016)

Measurement Tomography of QPG

quantifies quality of QPG for TM POVM measurements

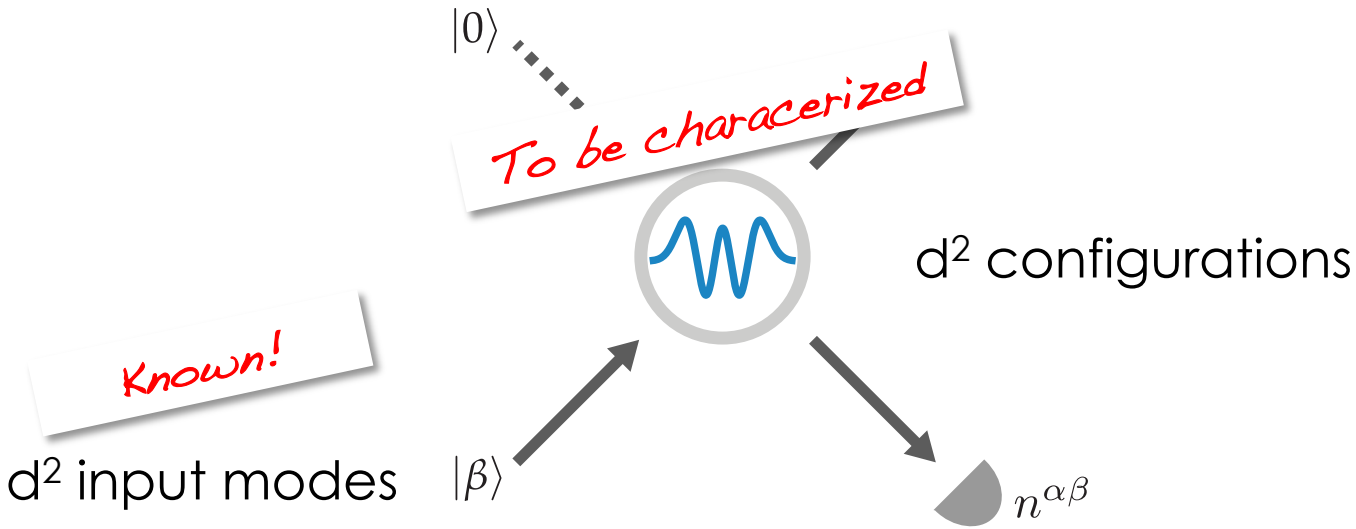

$$n^{\alpha\beta} = \mathrm{tr}(\hat{M}^{\alpha}\hat{\rho}^{\beta})$$

Ansari et al., arXiv:1702.03336 (2017), Ansari et al., arXiv:1607.03001 (2016)

Temporal-mode detector tomography

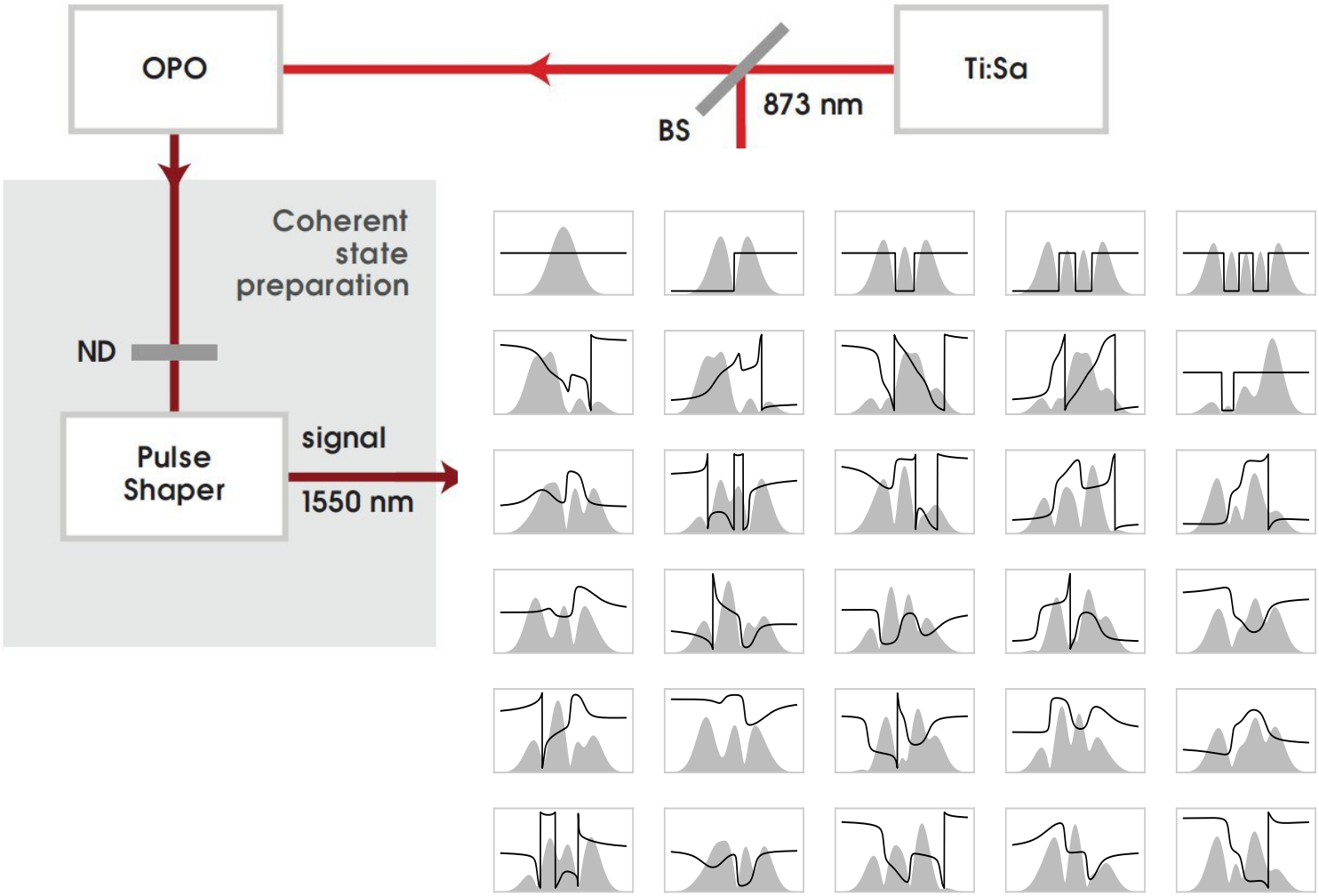

V. Ansari, G. Harder, M. Allgaier, B. Brecht, and C. Silberhorn. arXiv:1702.03336

Temporal-mode detector tomography

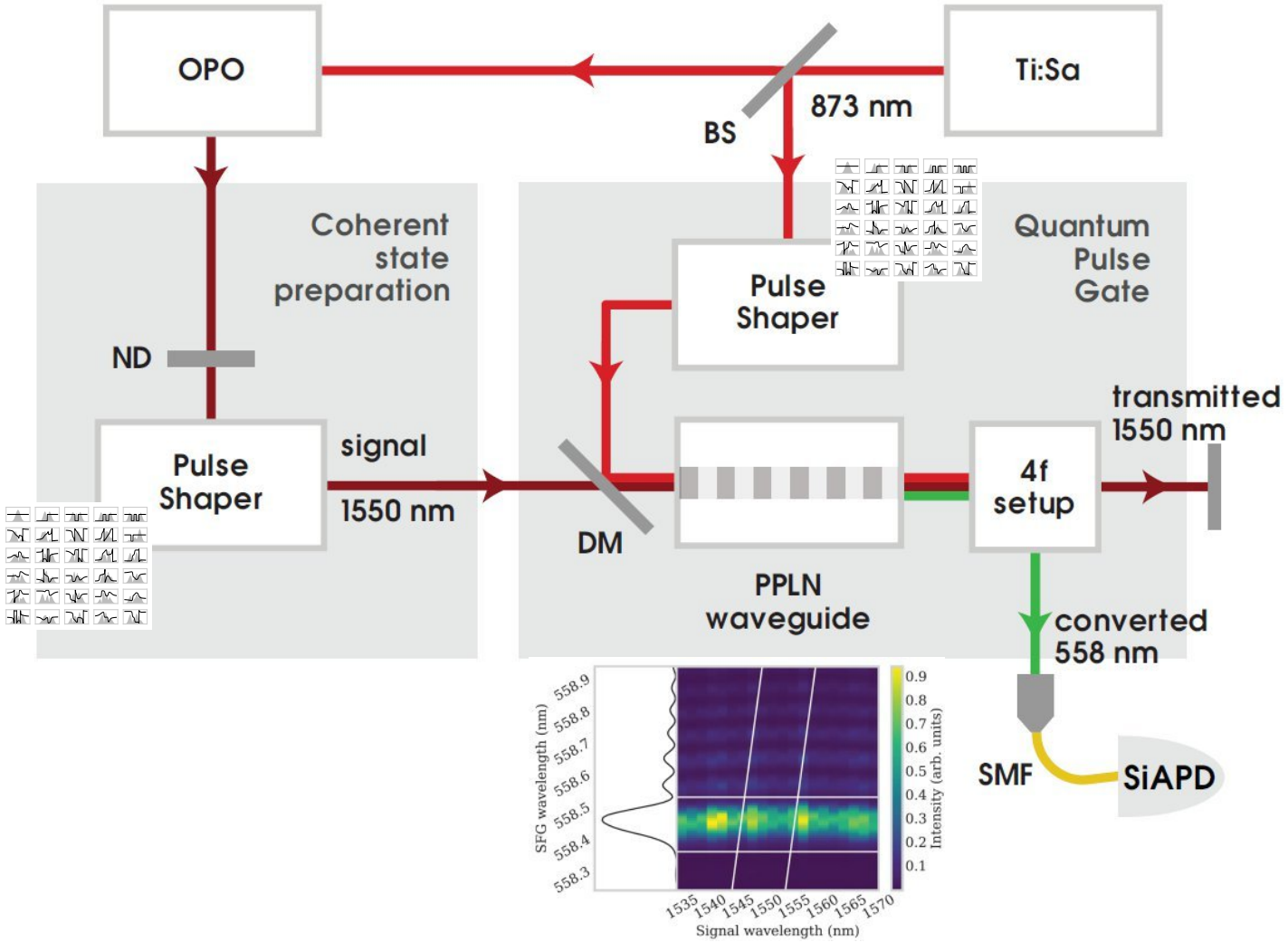

V. Ansari, G. Harder, M. Allgaier, B. Brecht, and C. Silberhorn. arXiv:1702.03336

Temporal-mode detector tomography

Ideal measurements

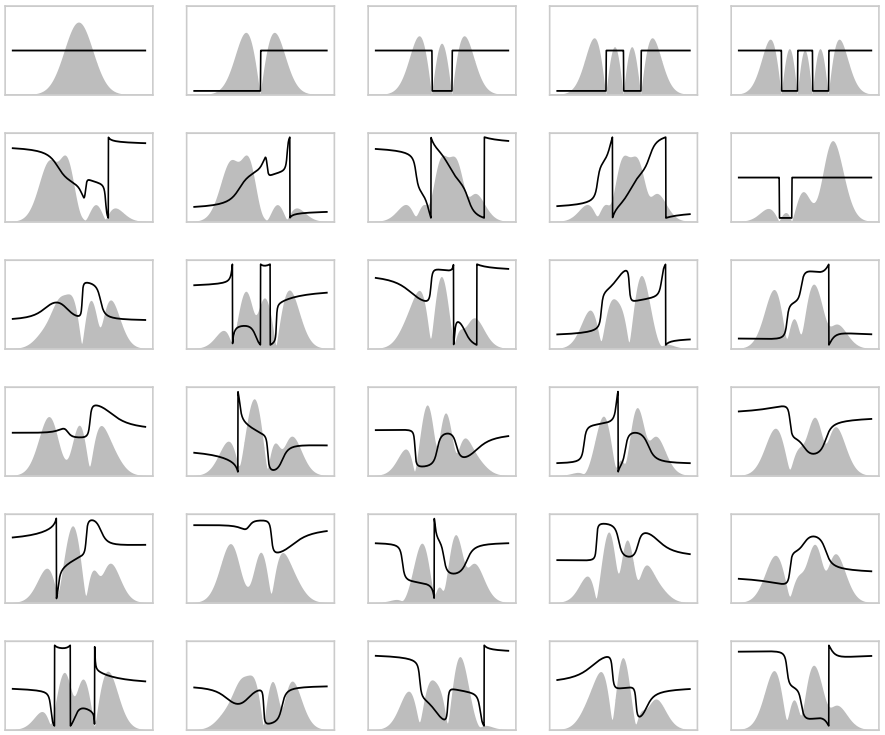

Characterized measurements

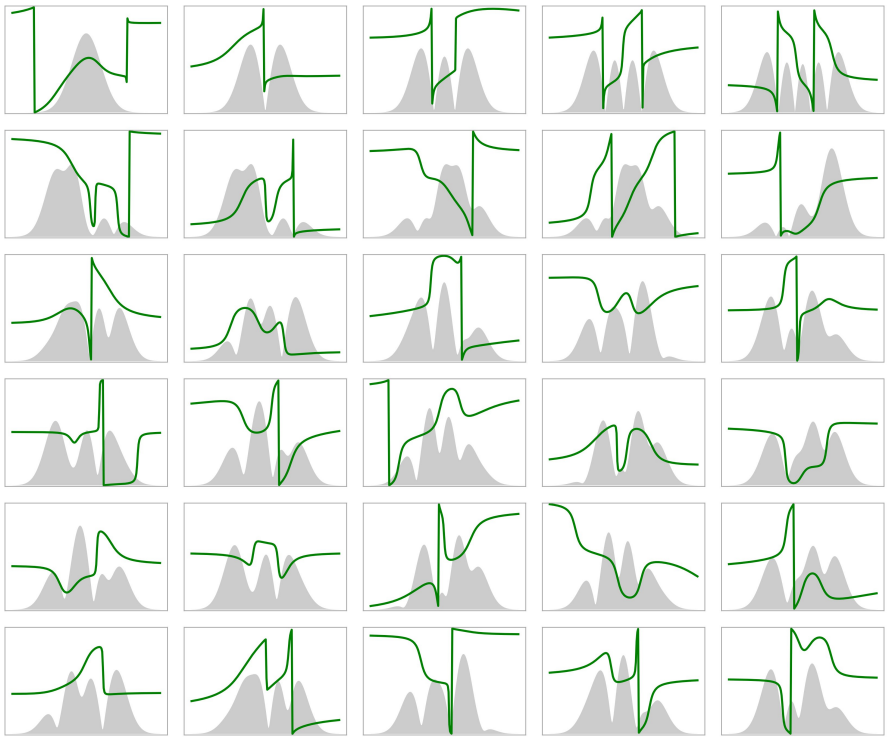

V. Ansari, G. Harder, M. Allgaier, B. Brecht, and C. Silberhorn. arXiv:1702.03336

Temporal-mode tomography

Test on shaped classical pulses

Dimension	Idealized projectors
5	87.9% ± 4.1%
7	81.3% ± 3.1%

Average fidelity of reconstructed temporal-mode density matrices

Theory

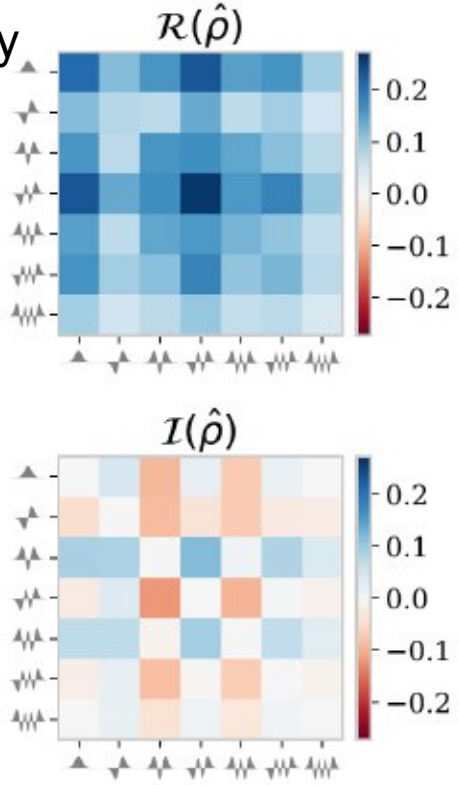

Experi-ment:

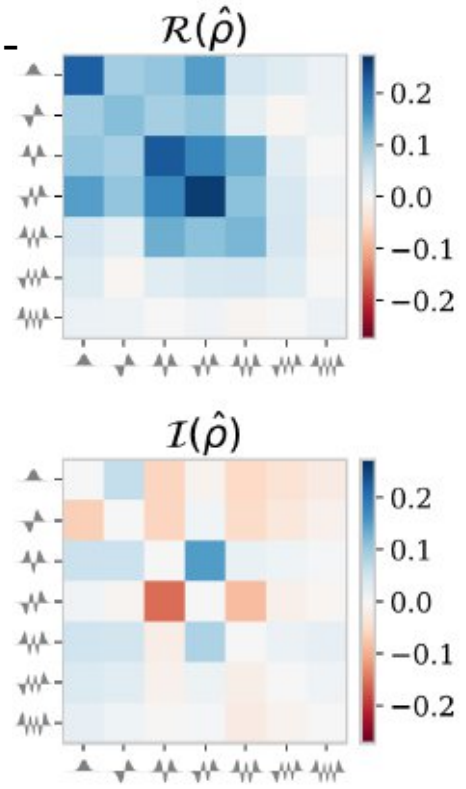

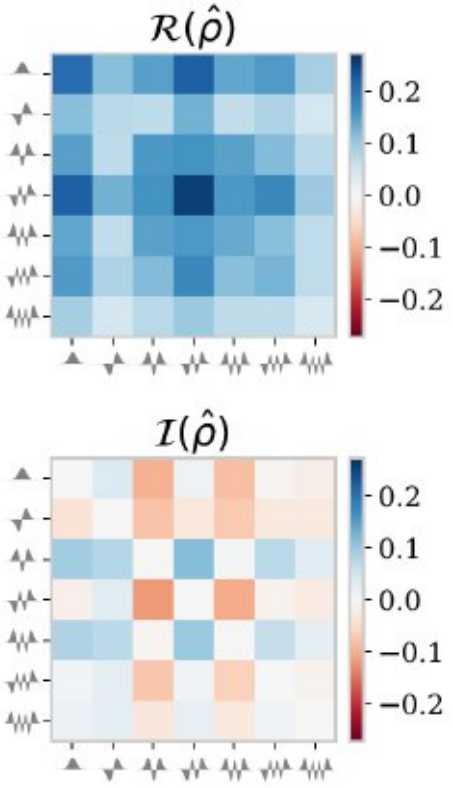

V. Ansari, G. Harder, M. Allgaier, B. Brecht, and C. Silberhorn. arXiv:1702.03336

Requirements for high dimensional quantum coding

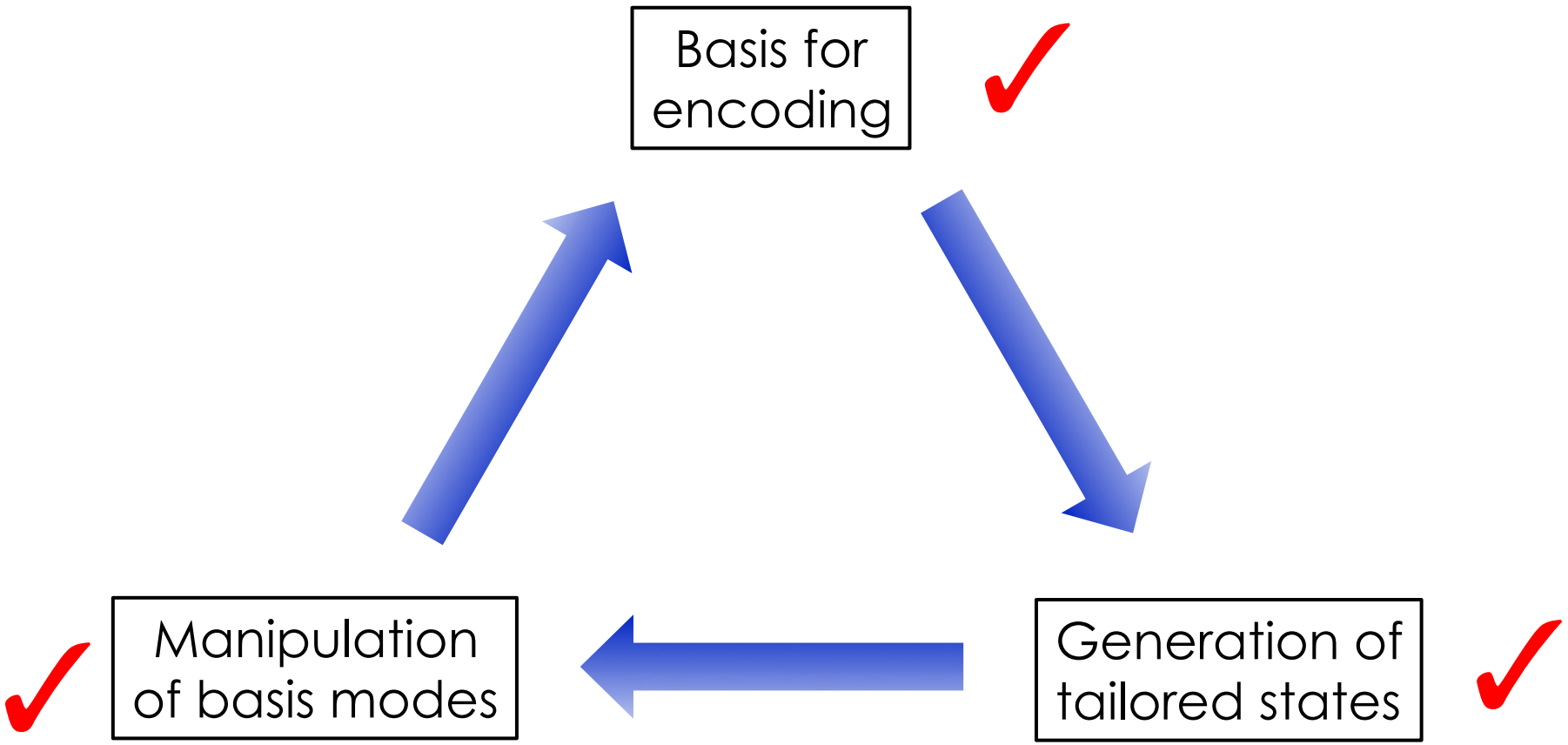

B. Brecht , D. V. Reddy, C. Silberhorn, M. G. Raymer, PRX **5**, 041017 (2015)

Outline

① Engineered parametric downconversion

② Quantum pulse gate

③ Applications

Temporal-mode tomography of PDC

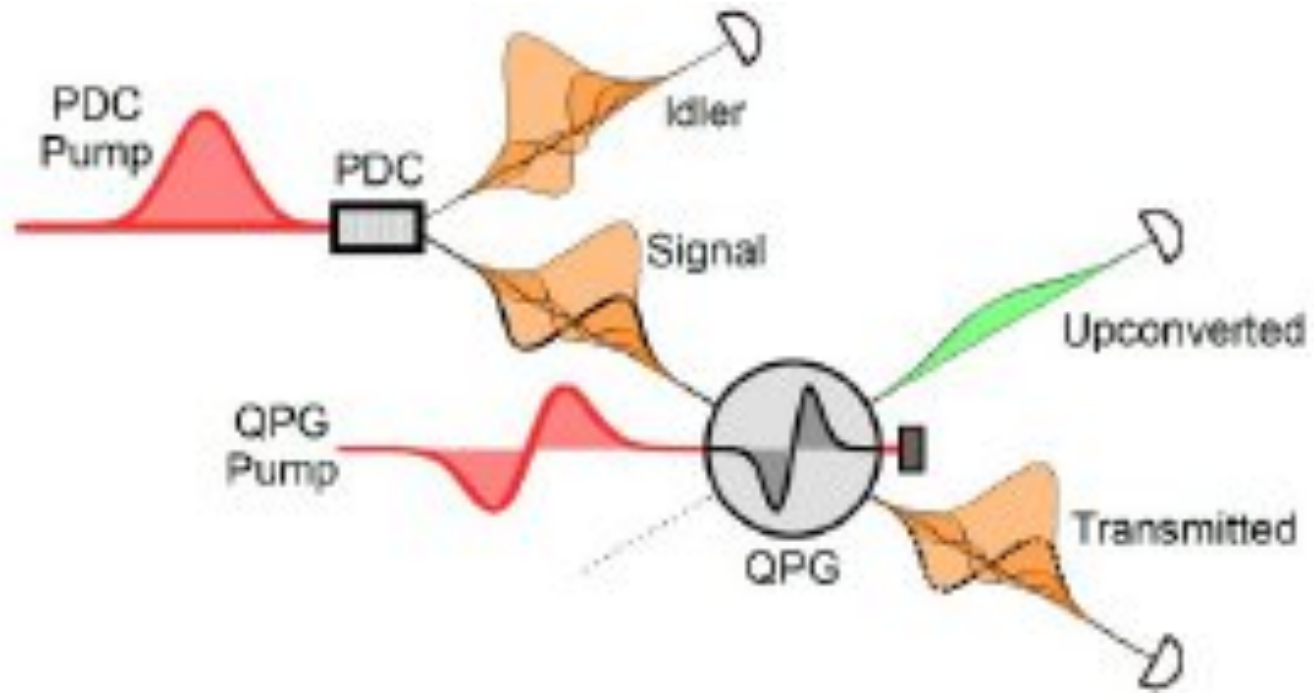

Temporal-mode tomography of PDC

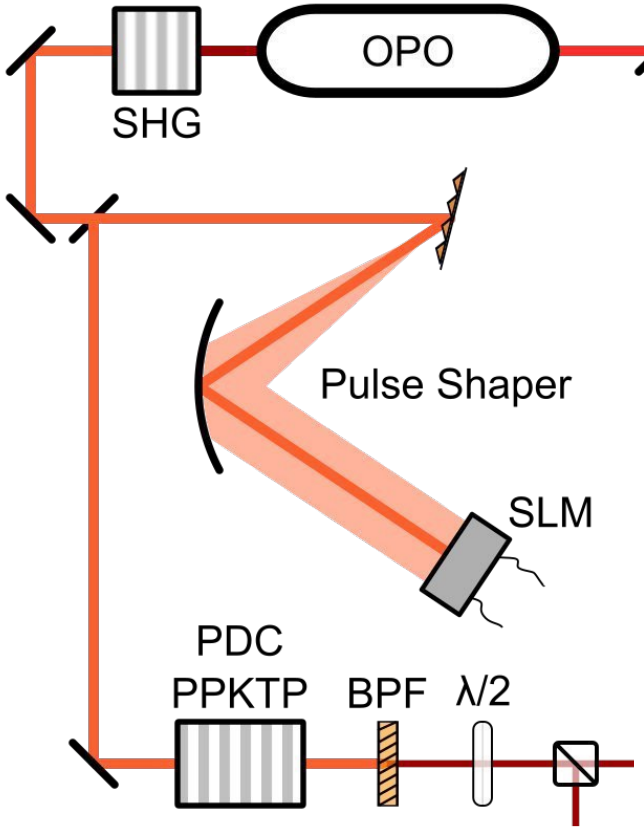

Extended phasematching

↓

Controllable time-frequency structure

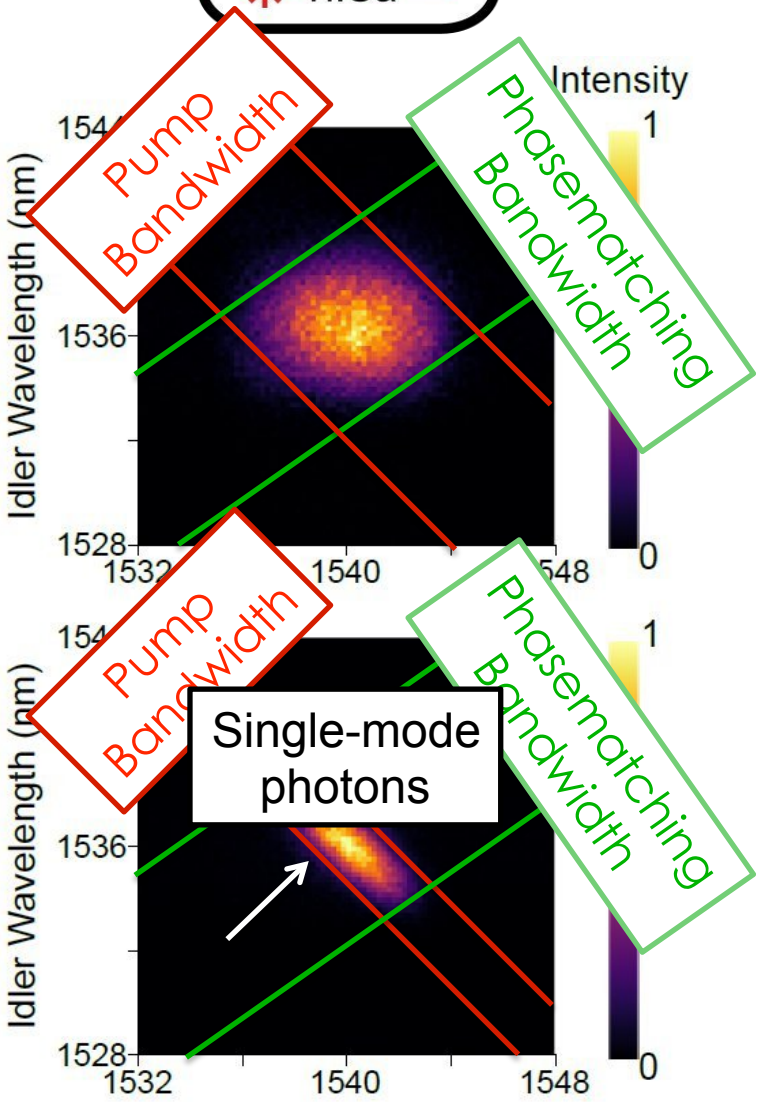

A. Eckstein et al., PRL **106**, 013603 (2011), arXiv:1006.5667; G. Harder et al., Opt. Express **21** 13975 (2013), arXiv:1304.6635

Temporal-mode tomography of PDC

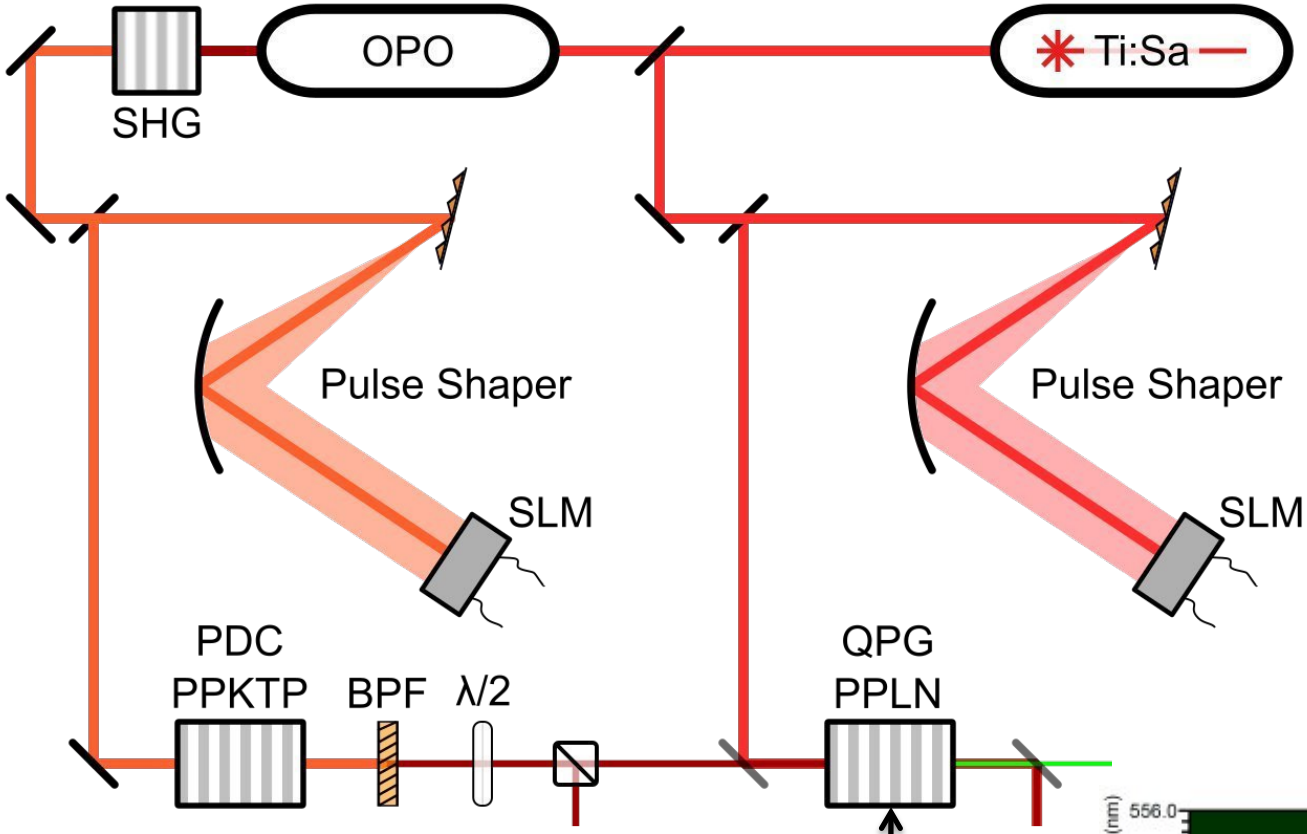

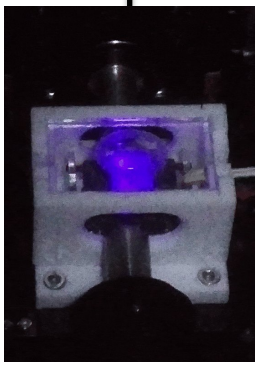

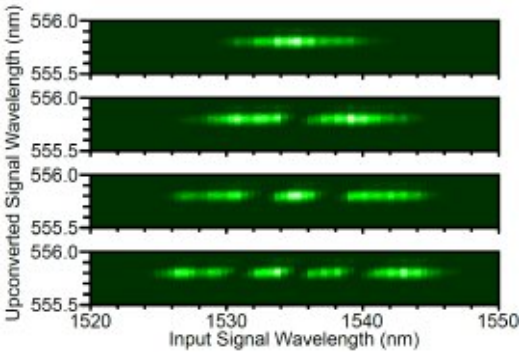

V. Ansari et al, arXiv:1607.03001v2 (2018)

Temporal mode tomography of PDC

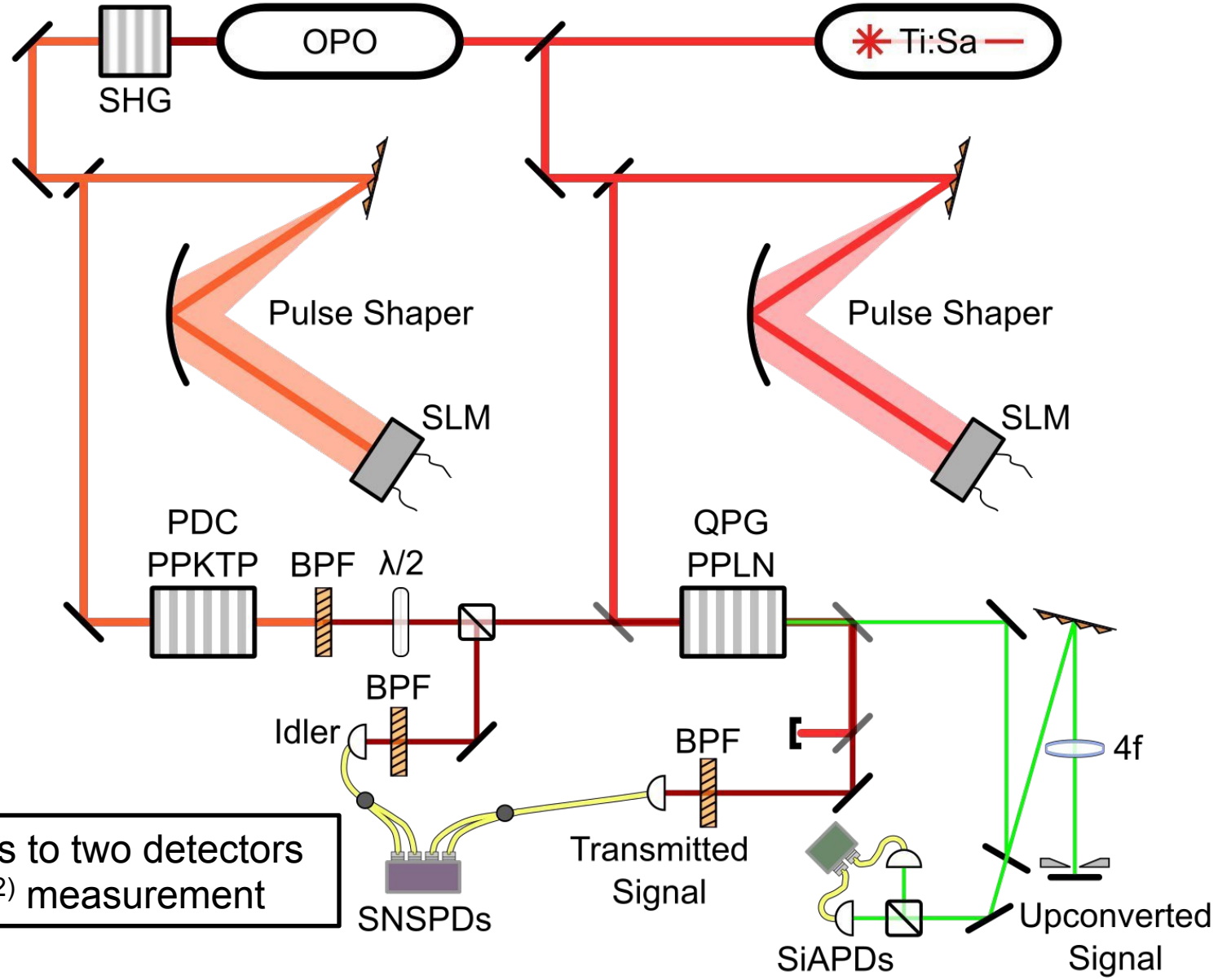

All paths to two detectors for $g^{(2)}$ measurement

V. Ansari et al, arXiv:1607.03001v2 (2018)

Purity from the $g^{(2)}$

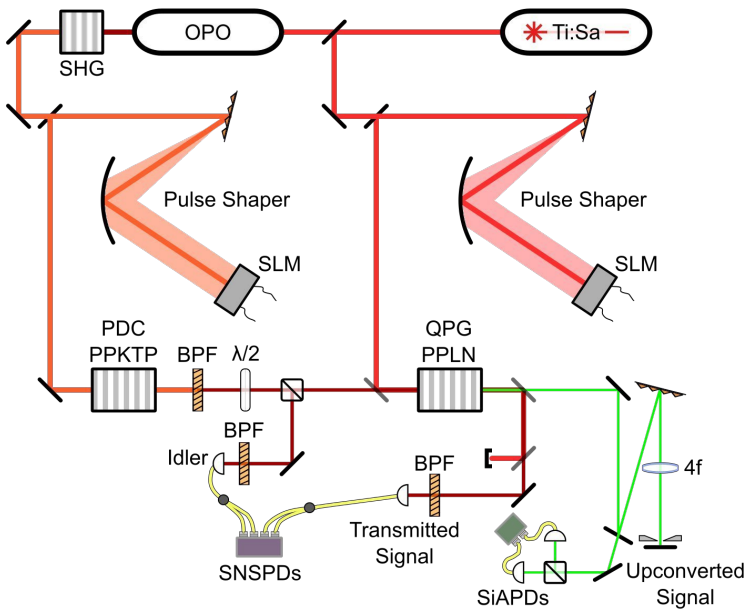

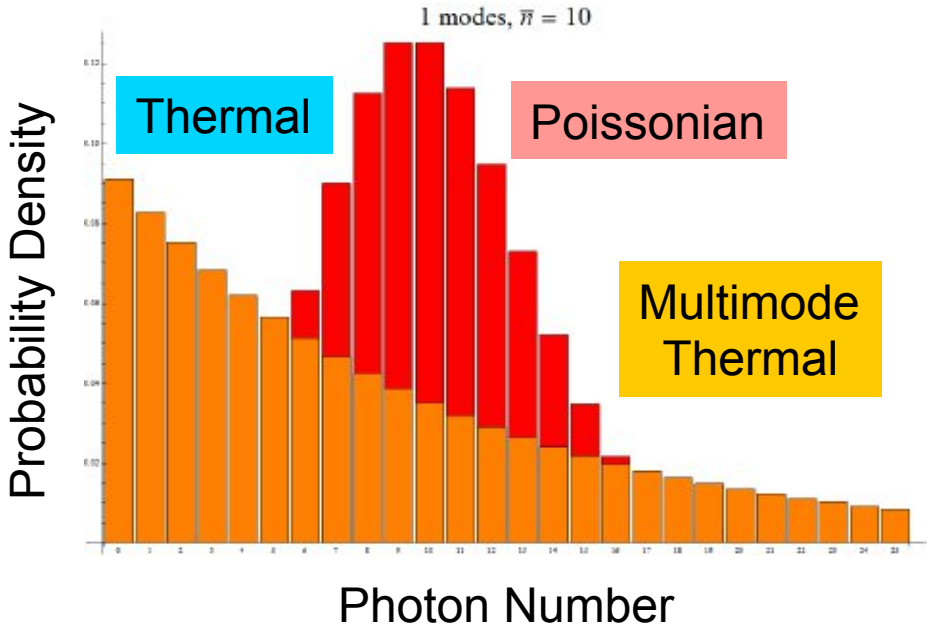

All paths to two detectors for $g^{(2)}$ measurement

Provides purity information independent of basis

Thermal $g^{(2)} = 2$

Poissonian $g^{(2)} = 1$

Multimode Thermal $g^{(2)} = 1 + \text{Purity}$

A. Christ et al., NJP **13** 033027 (2011), arXiv:1012.0262

Temporal-mode tomography of PDC

7-dimensional
tomographically complete set

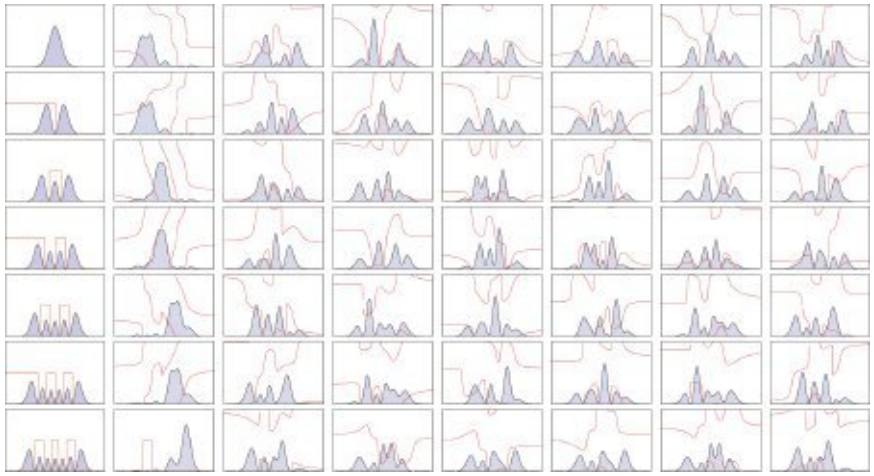

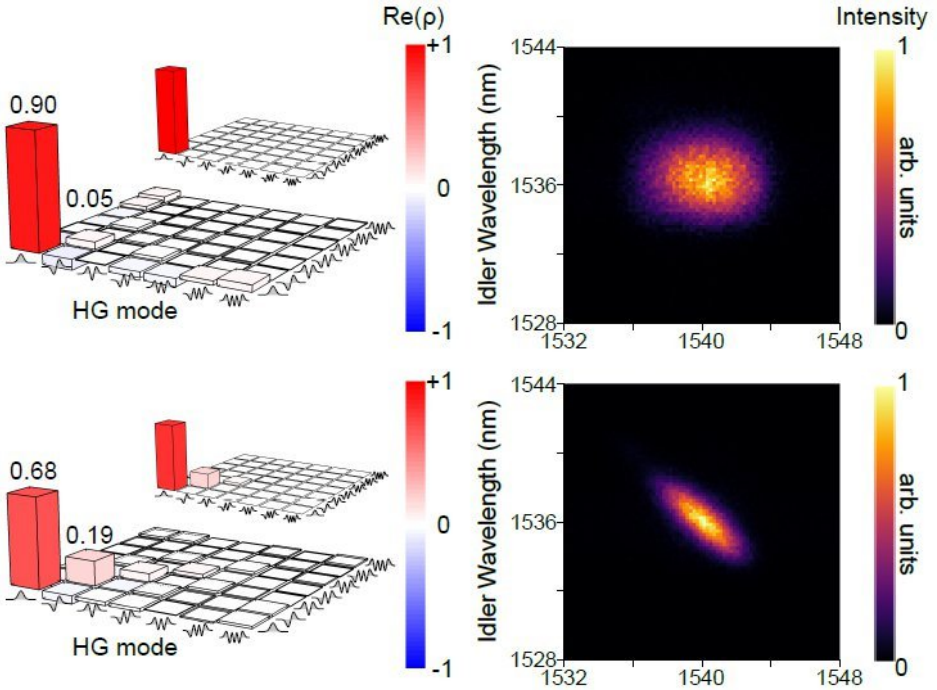

	Purity from $g^{(2)}$	Tomography
	0.929 ± 0.008	0.896 ± 0.008
	0.528 ± 0.010	0.523 ± 0.008

V. Ansari et al., arXiv:1607.03001v2 (2018)

Temporal-mode tomography of PDC

7-dimensional
tomographically complete set

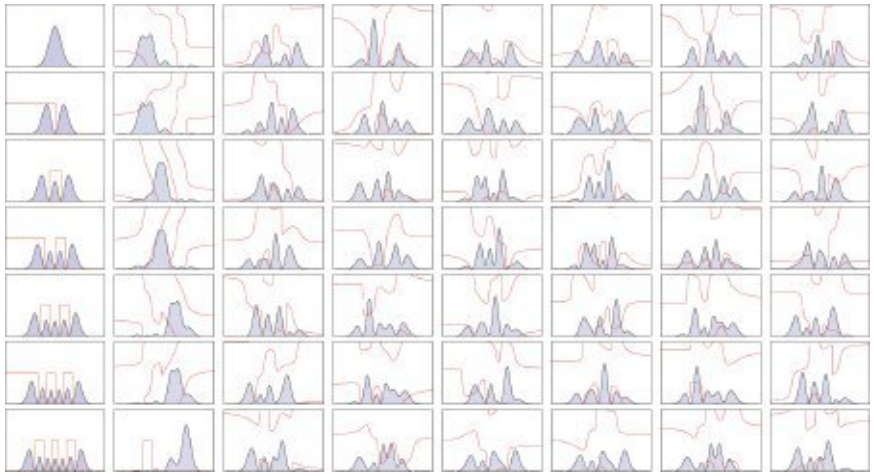

	Purity from $g^{(2)}$	Tomography
	0.929 ± 0.008	0.896 ± 0.008
	0.528 ± 0.010	0.523 ± 0.008
	0.327 ± 0.005	0.317 ± 0.005

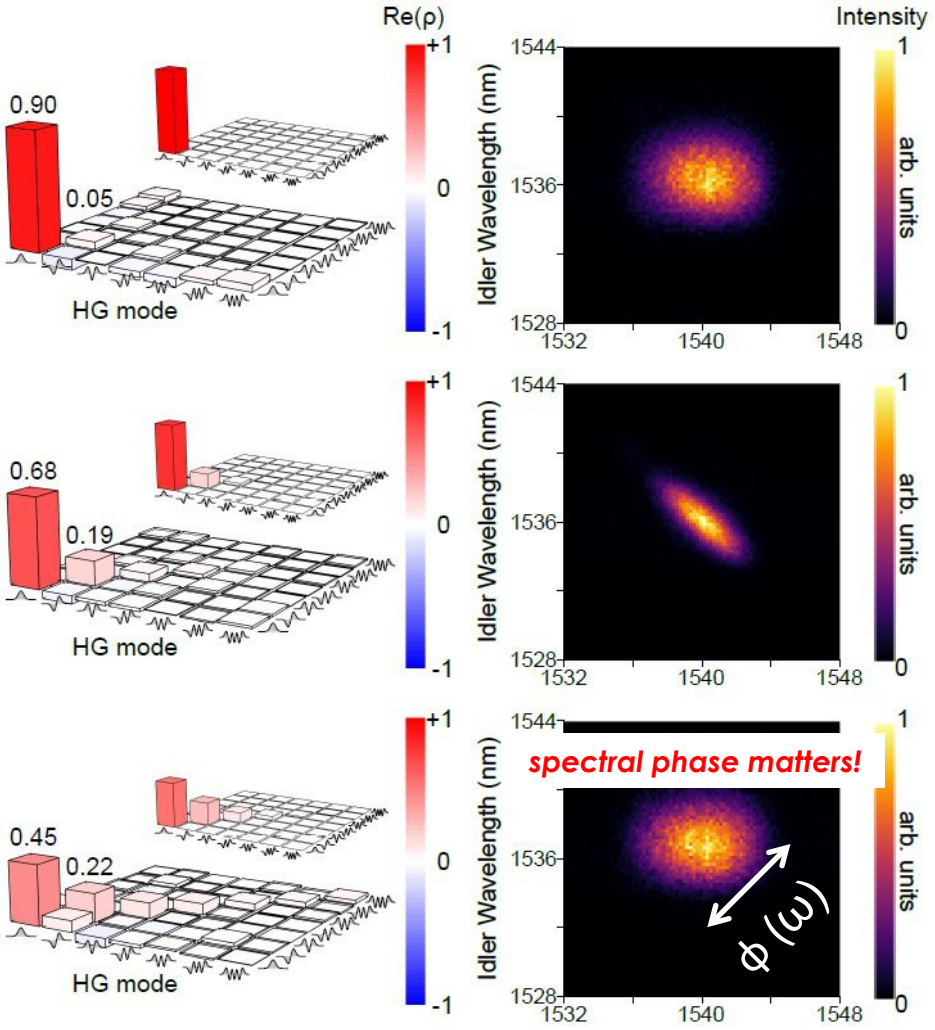

V. Ansari et al, arXiv:1607.03001v2 (2018)

TM tomography of single photons

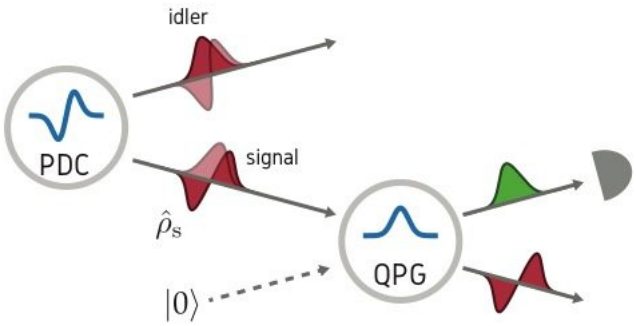

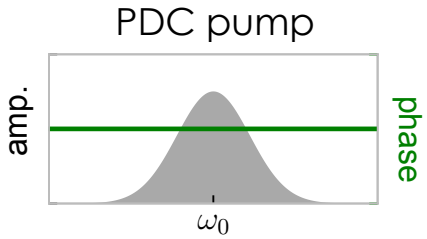

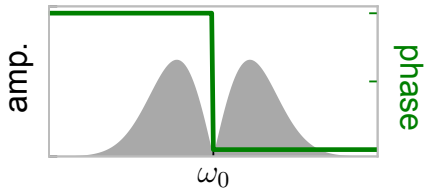

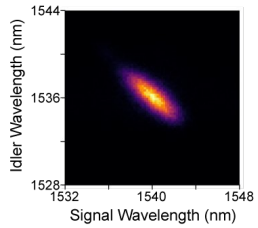

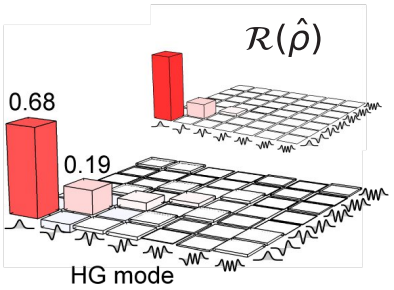

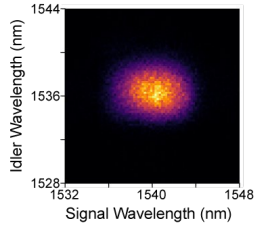

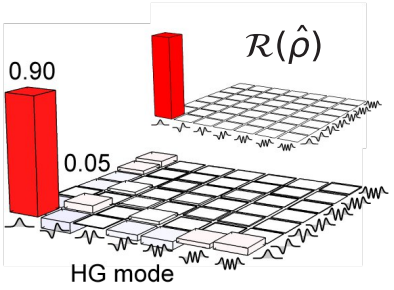

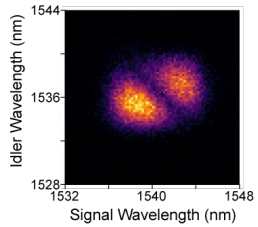

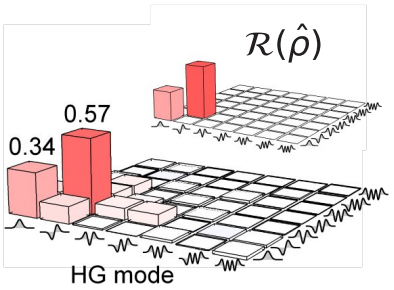

V. Ansari et al, arXiv:1607.03001v2 (2018)

Parameter estimation with incoherent emitters

Space

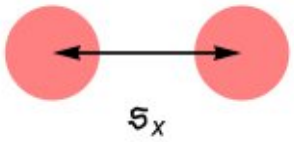

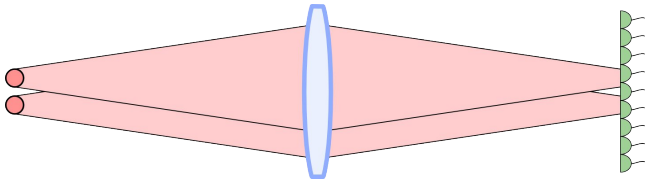

Frequency

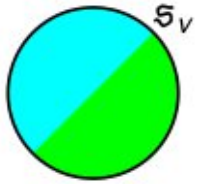

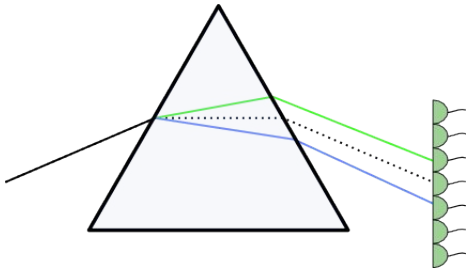

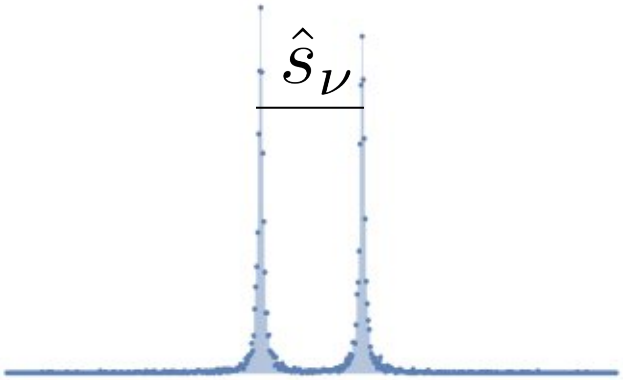

Time

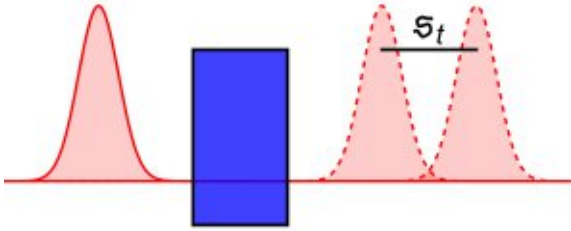

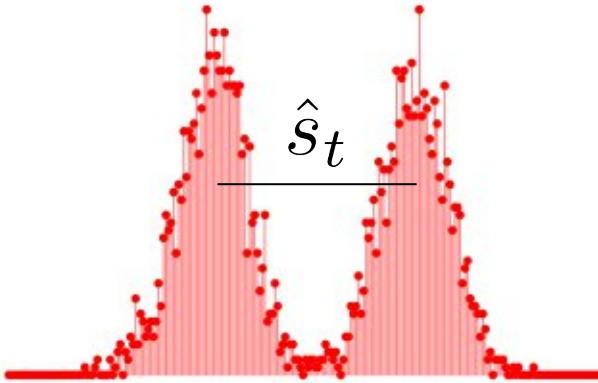

* Coherent A.P.E. PulseCheck Autocorrelator

Parameter estimation with incoherent emitters

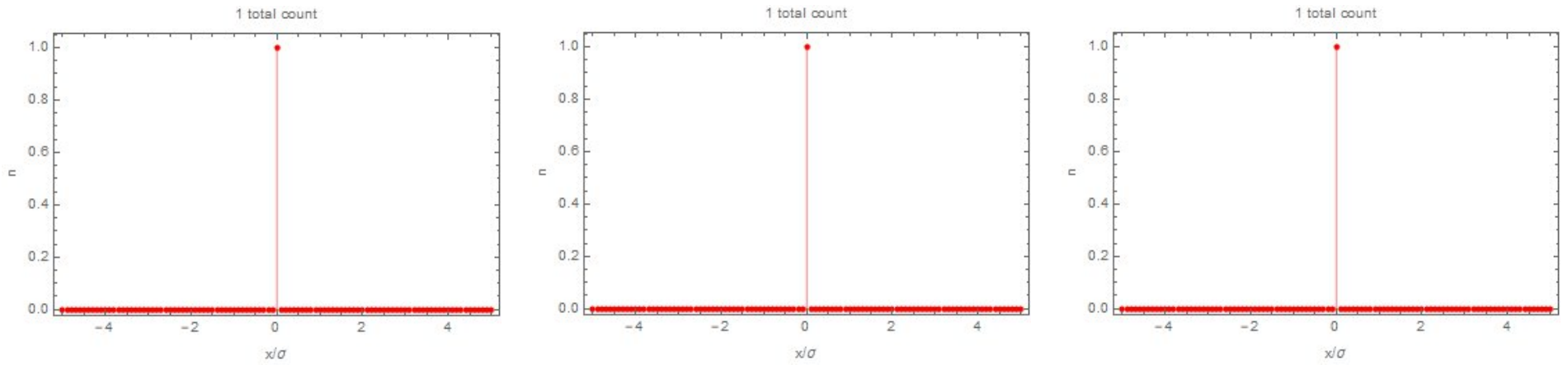

Rayleigh's Curse

$$\mathrm{Var}(\hat{s}) \geq \frac{1}{N \int \mathrm{d}x \, \frac{1}{I(x,s)} \left(\frac{\partial I(x,s)}{\partial s} \right)^2}$$

Intensity-Counting Limit

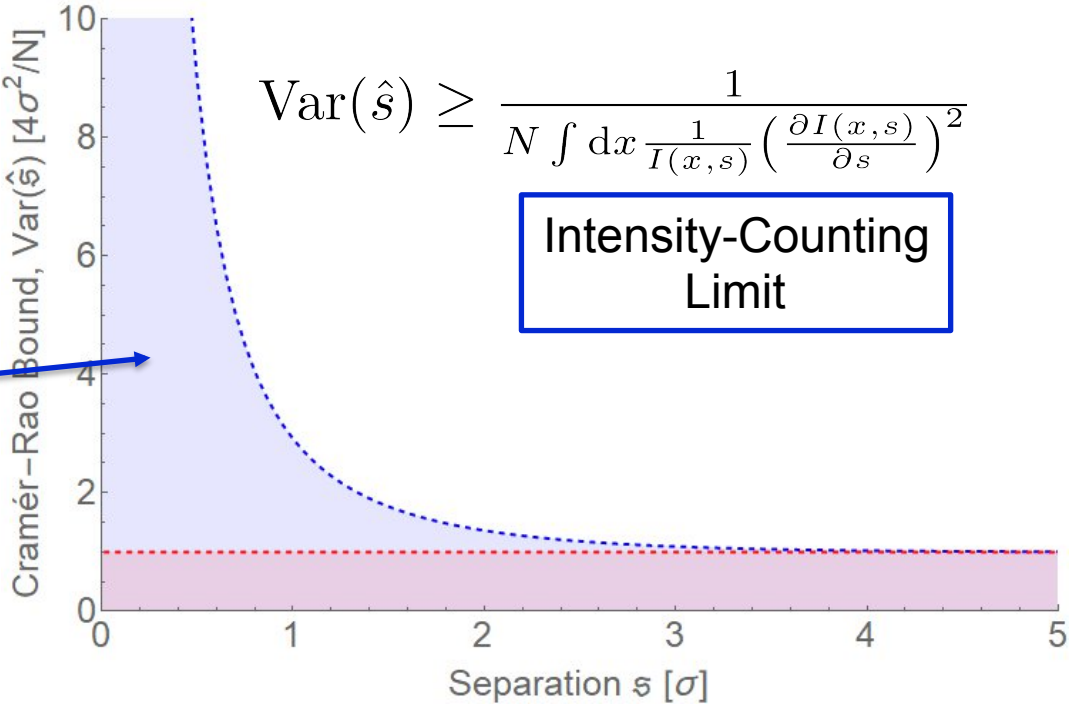

M. Tsang, R. Nair, and X.-M. Lu, Phys. Rev. X **6**, 031033 (2016).

Overcoming the curse

Mode selective measurement break the curse!

$$\mathrm{Var}(\hat{s}) \geq \frac{1}{N\int \mathrm{d}x \frac{1}{I(x,s)}\left(\frac{\partial I(x,s)}{\partial s}\right)^2} \geq \frac{1}{4N\sigma^2}$$

Intensity-Counting Limit

Quantum Limit

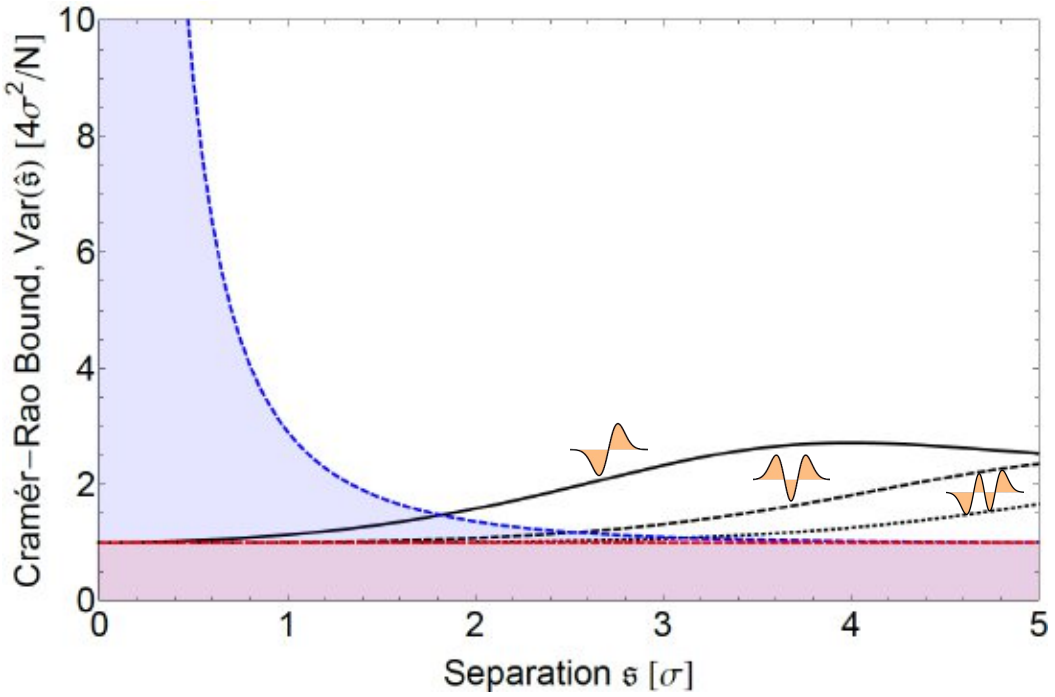

M. Tsang, R. Nair, and X.-M. Lu, Phys. Rev. X **6**, 031033 (2016).
M. Paur, B. Stoklasa, Z. Hradil, L.L. Sanchez-Soto, and J. Rehacek, Optica 3 1144 (2016)

Mode-selective measurement

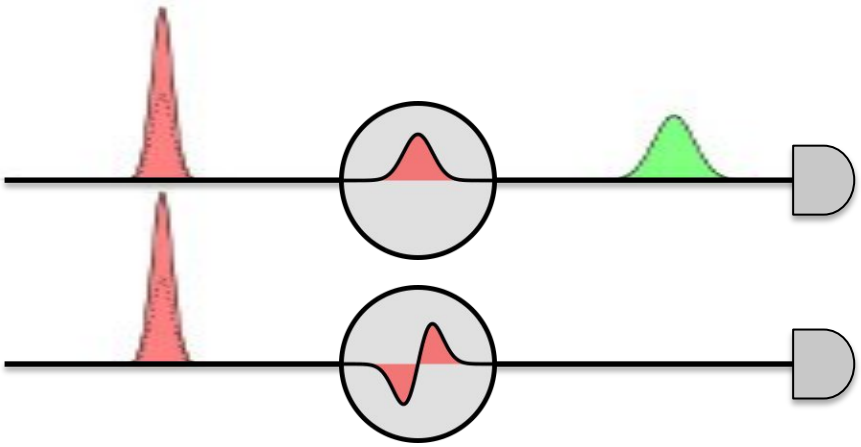

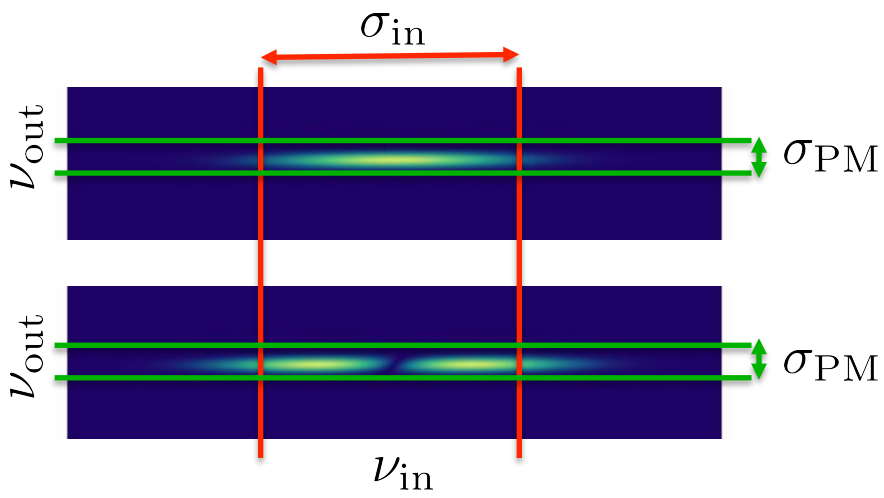

$$\frac{P_{\rm HG0}}{P_{\rm HG1}} = \frac{\sigma_{\rm in}^2}{\sigma_{\rm PM}^2} + \frac{s^2}{\sigma_{\rm in}^2}$$

Visibility	Estimator

Changes the time-frequency scale of the curse

Works equally well for time and frequency separations

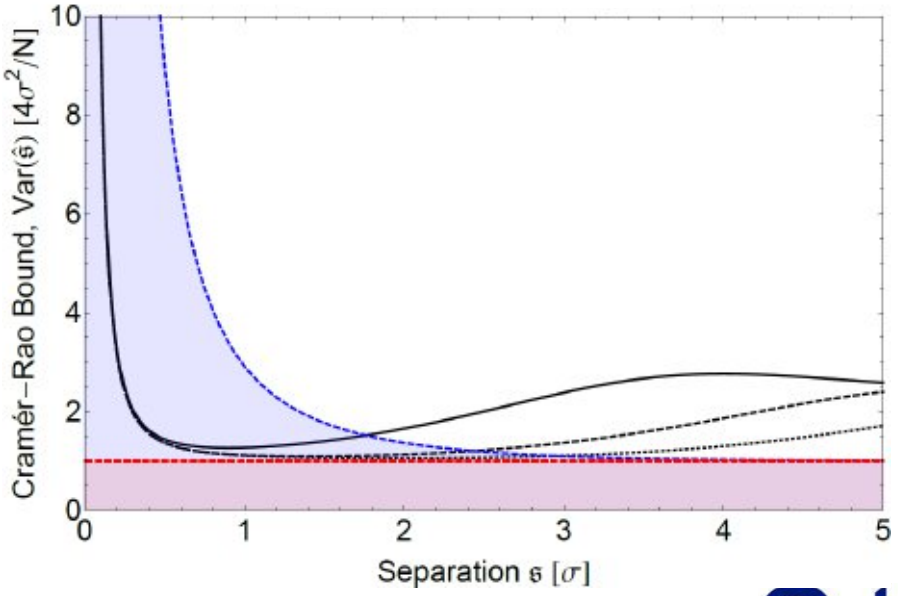

J.M. Donohue et al, arXiv:1805.02491

Experiment

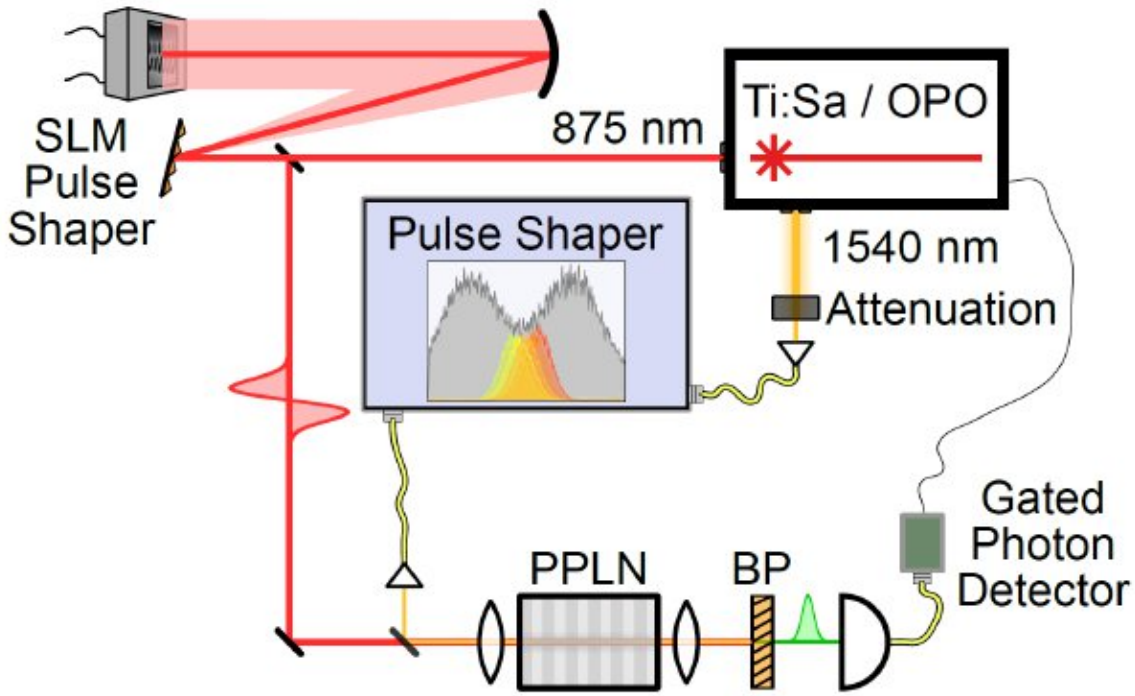

Lithium Niobate Type-II, 4.4μm poling
1540 nm + 875 nm → 558 nm

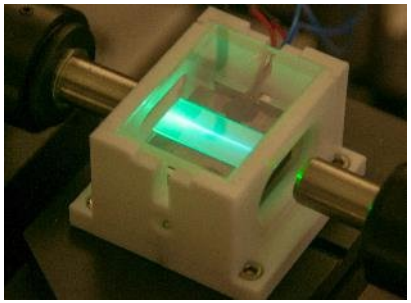

Group Velocity Matching

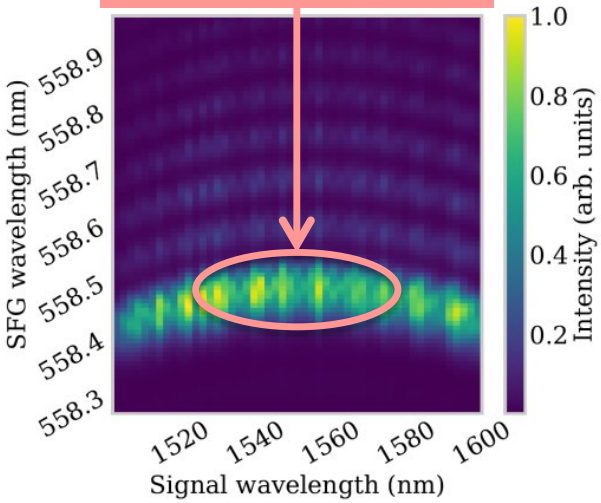

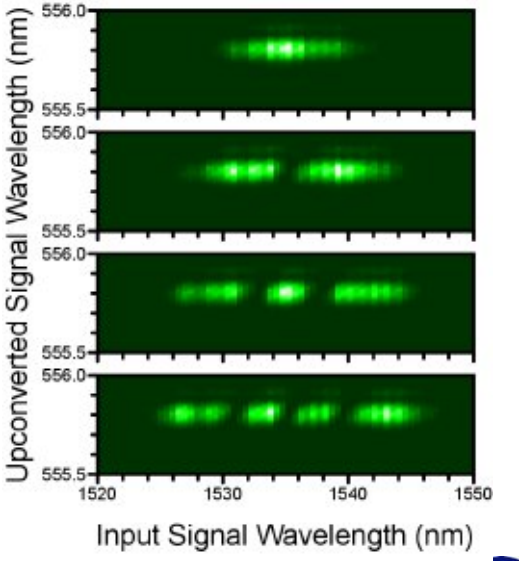

J.M. Donohue et al, arXiv:1805.02491

Results: Time-frequency estimation

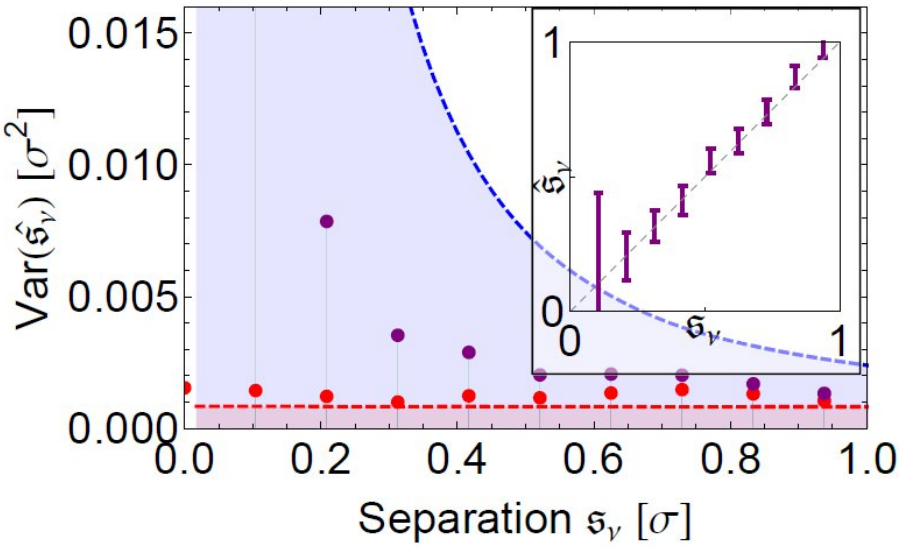

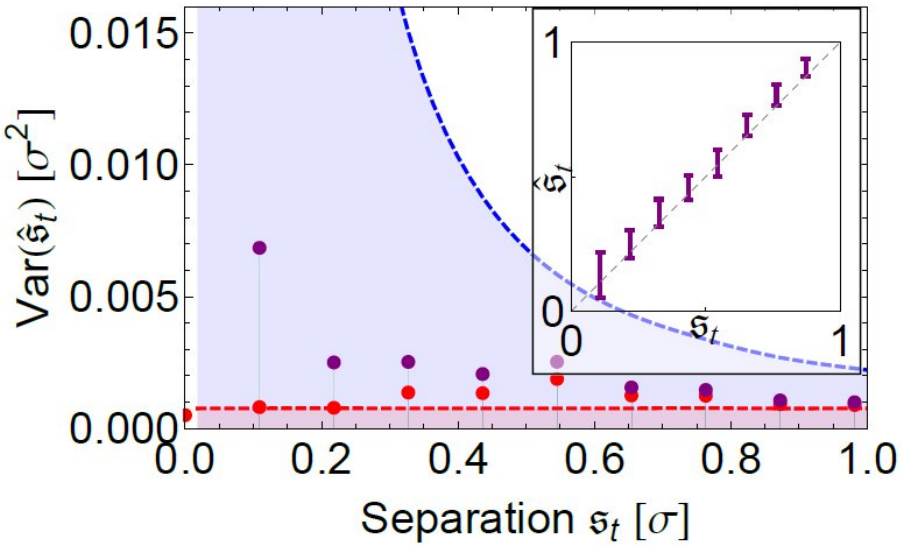

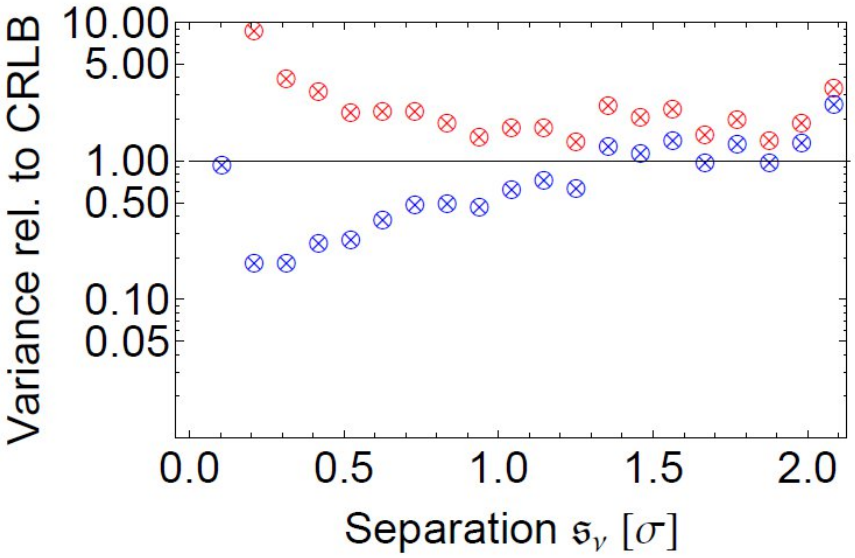

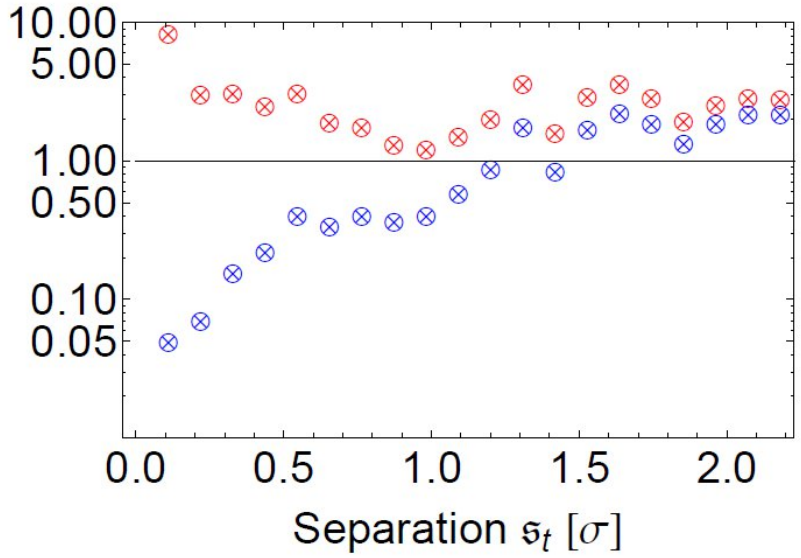

J.M. Donohue et al, arXiv:1805.02491

Conclusion

① Engineered parametric downconversi

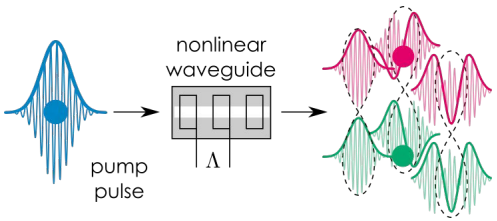

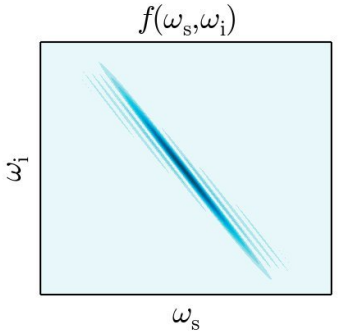

② Quantum pulse gate

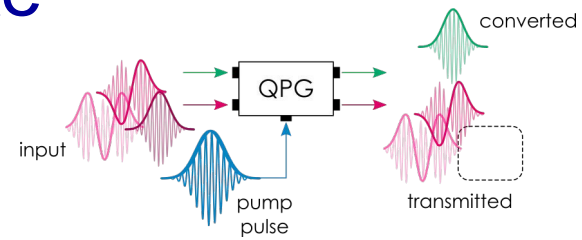

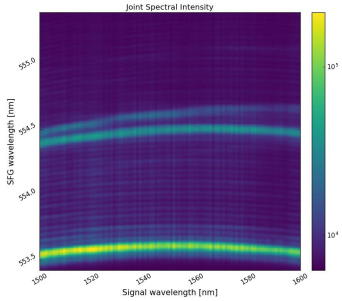

③ Applications

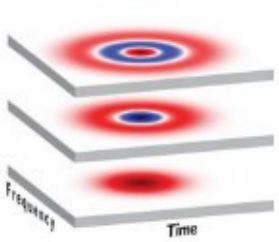

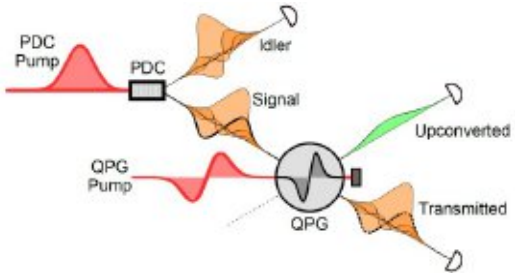

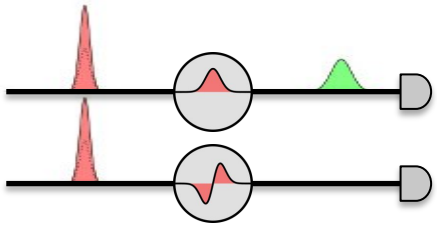

Thank you for your attention!

Deutsche Forschungsgemeinschaft DFG

UNIVERSITÄT PADERBORN
Die Universität der Informationsgesellschaft

SFB TRR 142

technische universität dortmund

erc
European Research Council
Established by the European Commission

QCUMbER

QUCHIP
Quantum Simulation on a Photonic Chip

PICQUE